Methods and Applications of Analysis
1 (3) 1994, pp. 314–347

ISSN 1073–2772

On perturbations of cubic fold points for nonlinear eigenvalue problems

Michael J. Ward and Sven A. Wolf

Dedicated to Chuck Lange

Abstract. We consider fold point behavior for nonlinear eigenvalue problems of the form

$$\triangle u_0 + \lambda_0 F(u_0, \beta) = 0, \quad x \in D; \quad \partial_\nu u_0 + b u_0 = 0, \quad x \in \partial D.$$

Here b and β are positive parameters. In circular cylindrical or spherical geometries, we assume that $F(u, \beta)$ is such that this problem has multiple radially symmetric solutions for some range of λ_0 only when $0 < \beta < \beta_0$. As $\beta \to \beta_0$ from below, two simple fold points are assumed to coalesce producing a cubic fold point at $\lambda_0 = \lambda_{c0}$ when $\beta = \beta_0$. We calculate the change in the cubic fold point location resulting from various classes of perturbations of this problem. The perturbations we consider are a small change in the boundary condition maintained on the boundary of a circular cylindrical or a spherical domain, a small distortion of the boundary of a circular cylindrical domain, and the removal of a small hole from a domain. In each case, we derive asymptotic expansions for the location of the perturbed cubic fold point in terms of a small parameter ϵ measuring the size of the perturbation. A numerical scheme is then formulated to evaluate the coefficients in these expansions and the method is illustrated for the combustion nonlinearity $F(u, \beta) = \exp[u/(1 + \beta u)]$. In certain cases, we compare our expansions for the perturbed cubic fold point location with some previous results and with results obtained from full numerical solutions to the perturbed problems. The significance of these results for the perturbed cubic fold point location are that they can provide the first step in characterizing, at least locally, the alteration of the boundary in parameter space that separates regions where the nonlinear eigenvalue problem has multiple solutions from regions where the problem has only unique solutions.

1. Introduction

We consider fold point behavior for nonlinear eigenvalue problems of the form

$$\triangle u_0 + \lambda_0 F(u_0, \beta) = 0, \quad x \in D, \tag{1.1a}$$

$$\partial_\nu u_0 + b u_0 = 0, \quad x \in \partial D, \tag{1.1b}$$

$$\alpha = \int_D u_0^2 \, dx. \tag{1.1c}$$

Received September 17, 1993, revised March 12, 1994.
1991 *Mathematics Subject Classification*: 35B32, 35C20.
Key words and phrases: cubic fold point, domain and temperature perturbations, asymptotic expansions, infinite logarithmic expansions, combustion nonlinearity, extended systems.
The first author was partially supported by the NSERC grant 5-81541 and by the Applied Mathematical Sciences Program of the U.S. Dept. of Energy under contract DE-FG02-88ER25053.

Here b is a positive constant, λ_0 is the nonlinear eigenvalue parameter, β is a positive parameter, D is a bounded two- or three-dimensional domain, and ∂_ν is the outward normal to ∂D. The nonlinearity $F(u, \beta)$ is taken to be such that for fixed β in some neighborhood of the origin, multiple solutions to (1.1) occur for some range of λ_0. More specifically, we assume that when β satisfies $0 < \beta < \beta_0$, the graph of α versus λ_0 is multiple-valued and has at least two simple fold points. We assume that this solution branch can be parameterized as $u_0 = u_0(x, \alpha, \beta)$ and $\lambda_0 = \lambda_0(\alpha, \beta)$. As β tends to the critical value $\beta_0 = \beta_0(b)$, two simple fold points are assumed to coalesce producing a higher-order cubic fold point.

In circular cylindrical or spherical domains, the radially symmetric solution branch associated with the combustion nonlinearity $F(u, \beta) = \exp[u/(1 + \beta u)]$ leads to a response diagram with these types of qualitative properties (cf. [3], [4], [5]). In the combustion context, this form of F is the Arrhenius heating term and u_0 is the temperature of an exothermically active solid material in the absence of reactant consumption. Moreover, b is the dimensionless Biot number, $\beta \geq 0$ is the dimensionless activation energy parameter and λ_0 is the Frank-Kamenetskii parameter (cf. [6]). For this form of F, the behavior of radially symmetric solutions to (1.1) has been extensively studied in circular cylindrical and spherical geometries. For these geometries, it is well-known that a β_0 exists such that when $\beta < \beta_0$, multiple solutions to (1.1) can occur for some range of λ_0 (cf. [3], [4], [5]). Alternatively, when $\beta > \beta_0$, solutions to (1.1) exist and are unique for all $\lambda_0 > 0$. When $0 < \beta < \beta_0$, the response diagram α versus λ_0 for a circular cylindrical domain is S-shaped with two simple (or quadratic) fold points at $\lambda_{0-} \equiv \lambda_0(\alpha_-, \beta)$ and $\lambda_{0+} \equiv \lambda_0(\alpha_+, \beta)$. The determination of the critical value λ_{0+}, which connects the lower and middle branches of the response diagram, is important in reactor design in that as λ_0 increases past λ_{0+}, a dramatic rise in the temperature will occur (i.e., a thermal explosion). In contrast, the response diagram α versus λ_0 for a spherical domain has many simple fold points when β is small (cf. [3]). However, when β is sufficiently close to β_0 the response diagram for a spherical domain has the same S-shaped form as that for a circular cylindrical domain (see Figure 1).

Thus, for circular cylindrical and spherical geometries, criticality is lost as β approaches β_0 through the coalescence of two simple fold points producing a cubic fold point when $\beta = \beta_0$. We denote the values of α and λ_0 at this cubic fold point by α_0 and $\lambda_{c0} = \lambda_0(\alpha_0, \beta_0)$. The values α_0, β_0, and λ_{c0} are then referred to as the unperturbed cubic fold point parameters. For the combustion nonlinearity, these parameters have been computed numerically for circular cylindrical and spherical geometries over a wide range of Biot number b (cf. [9], [5], [7], [4]).

For classes of nonlinearity $F(u, \beta)$ where (1.1) admits multiple solutions, there have been some recent studies (cf. [1], [11], [13], [14], [16]) devoted to characterizing the sensitivity of a simple fold point to various classes of perturbations of (1.1). Specifically, for various perturbed forms of (1.1), asymptotic expansions for the location of the perturbed simple fold point have been derived. When applied to the combustion nonlinearity $F(u, \beta) = \exp[u/(1 + \beta u)]$, these expansions quantify the change in the conditions for the onset of thermal runaway as a result of perturbations in the domain geometry or non-uniform temperature perturbations maintained on the boundary of the domain. For the case $F = e^u$, the conditions for the onset of thermal runaway in a nearly circular domain were determined in [1]. These results were extended in [13] to allow for a large class of nonlinearities. In [13], the effect on a simple fold point of a temperature perturbation maintained on the boundary of a circular cylindrical domain was also considered. Simple fold point behavior associated with removing a

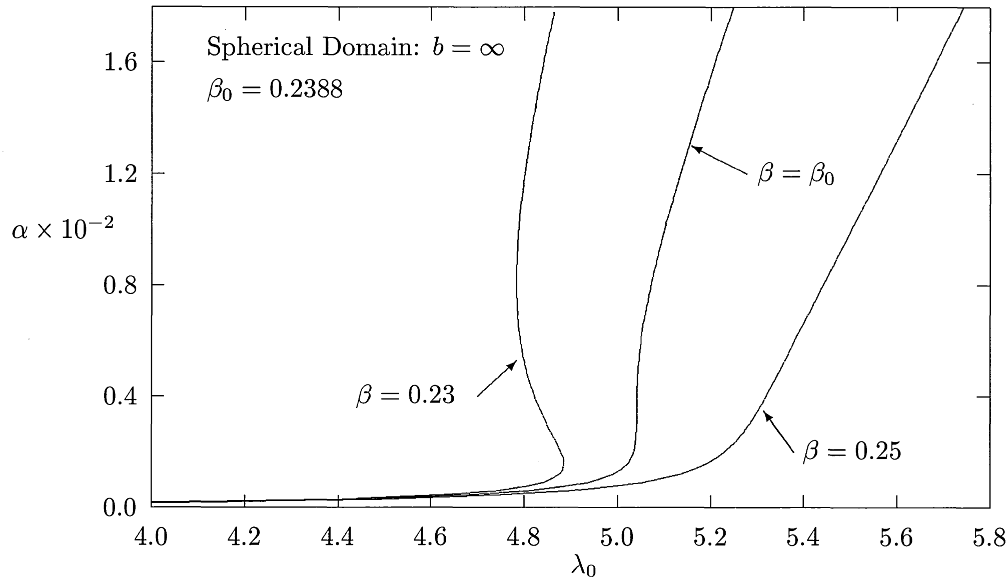

FIGURE 1. Spherical domain with radius one and $b = \infty$: Plots of α versus λ_0 for three values of β with $\beta \approx \beta_0 = .2388$.

small arbitrarily shaped hole from a two- or three-dimensional domain was analyzed in [13] and [16]. A similar problem was considered in [11] for a concentric circular cylindrical geometry.

Our goal in this paper is to extend this previous work on perturbations of simple fold points in order to determine the sensitivity of the location of a cubic fold point for (1.1) to various classes of perturbations. In particular, we analyze the effect on the cubic fold point of a perturbation in the boundary condition that is maintained on the boundary of a circular cylindrical or a spherical domain. We also consider the effect of both regular and singular perturbations of the domain geometry. Specifically, we analyze the case of a small distortion of the boundary of a circular cylindrical domain and the case of the removal of a small subdomain from an arbitrary two- or three-dimensional domain with a condition imposed on the boundary of the resulting hole. For each class of perturbation, we use asymptotic and bifurcation methods to construct asymptotic expansions for the location of the perturbed cubic fold point in terms of a small parameter ϵ measuring the size of the perturbation. A key feature of the analysis is that very similar methods can be used to treat the diverse classes of perturbed problems. The significance of the asymptotic results for the perturbed cubic fold point is that they can provide the first step in characterizing, at least locally, the alteration of the boundary in the (λ, β) parameter space that separates regions where (1.1) has multiple solutions from regions where (1.1) has unique solutions.

For problems where the unperturbed domain is a circular cylinder or a sphere, we will formulate a method to evaluate certain coefficients in the asymptotic expansions of the cubic fold point parameters. This method requires the numerical solution of an extended system of boundary-value problems subject to side constraints. The method then is used to evaluate the coefficients numerically for the combustion nonlinearity $F(u, \beta) = \exp[u/(1 + \beta u)]$. Although our results are illustrated only for this form of F, we emphasize that the asymptotic expansions for the cubic fold point parameters and the numerical method used to evaluate the coefficients in these expansions applies to an arbitrary F associated with cubic fold point behavior.

Some previous work on cubic fold point behavior in singularly perturbed domains is that of Lange and Weinitschke [11]. They considered the special case of a concentric circular cylindrical geometry with $u = 0$ on the small inner radius ϵ. For this geometry, they showed that the parameters defining the perturbed cubic fold point have asymptotic expansions in powers of $-1/\log \epsilon$. For the combustion nonlinearity $F(u, \beta) = \exp[u/(1 + \beta u)]$, they also gave numerical values for the first three terms in the logarithmic series for the cubic fold point parameters. We will extend this previous result to the case of a small hole of *arbitrary* shape centered at the origin with a more general condition imposed on the boundary of the hole. For this problem, the perturbed cubic fold point parameters have infinite-order logarithmic expansions in powers of $-1/\log[\epsilon d]$, where d is a constant determined by the hole geometry and the boundary condition on the hole. We then formulate a numerical method to sum these infinite logarithmic series and we illustrate the method for the combustion nonlinearity. A related method was formulated and used in [15] to sum a similar logarithmic series for the location of a simple fold point for (1.1a) in the same singularly perturbed geometry. We remark that infinite-order logarithmic expansions also occur for some singularly perturbed linear eigenvalue problems (cf. [15]) and in certain low Reynolds number fluid flow problems (cf. [8], [12]). The previous results of [11] for the cubic fold point location are also extended to the case where the small hole is off-center and has arbitrary shape. For this geometry, we derive a two-term expansion for the perturbed cubic fold point parameters. Similar results also are obtained for the three-dimensional case.

This paper is organized as follows. In §2 and §3, we analyze the effect of a perturbation in the boundary condition maintained on the boundary of a circular cylindrical or a spherical domain. In §4, we consider the effect of a small distortion of a circular cylindrical domain. In §5, we analyze the effect of a singular domain variation in which a small subdomain is removed from an arbitrary two- or three-dimensional domain. The results of §5 are then applied in §6 to circular cylindrical or spherical domains containing a small hole. For a cylindrical domain containing a small but arbitrarily shaped hole centered at the origin, in §6.2 we give a hybrid asymptotic-numerical method to sum the logarithmic expansions that define the cubic fold point. The analytical results of §3, §4, and §6 are illustrated for the combustion nonlinearity. For this form of F and for concentric spherical or circular cylindrical domains with small inner radius ϵ, in §6 we compare the asymptotic results for the location of the cubic fold point with full numerical results.

2. Small temperature variation on the boundary

The perturbed problem in dimensions $m = 2, 3$ is formulated as

$$\Delta u + \lambda F(u, \beta) = 0, \quad x \in D, \tag{2.1a}$$

$$\partial_\nu u + b\big(u - \epsilon h(s)\big) = 0, \quad x \in \partial D, \tag{2.1b}$$

where D is a bounded domain in R^m. The function $\epsilon h(s)$ represents the effect of a small specified external temperature perturbation and $s \in S \subset R^{m-1}$ is a parameterization of ∂D. We assume that we can write the solutions to (2.1) in the parametric form $u(x, \alpha, \beta, \epsilon)$, $\lambda(\alpha, \beta, \epsilon)$ where α is some measure of the norm of u. A convenient choice for α that we shall use here is

$$\alpha = \int_D u^2\, dx. \tag{2.1c}$$

We assume that the unperturbed problem (1.1) has a cubic fold point at the parameter values α_0, β_0, and $\lambda_{c0} \equiv \lambda_0(\alpha_0, \beta_0)$. We now determine the changes in these unperturbed cubic fold point parameters as a result of the temperature perturbation given in (2.1b).

For fixed α, we seek the solution to (2.1) for $\epsilon \ll 1$ in the form

$$u(x,\alpha,\beta,\epsilon) = u_0(x,\alpha,\beta) + \epsilon u_1(x,\alpha,\beta) + \epsilon^2 u_2(x,\alpha,\beta) + \cdots, \tag{2.2a}$$

$$\lambda(\alpha,\beta,\epsilon) = \lambda_0(\alpha,\beta) + \epsilon\lambda_1(\alpha,\beta) + \epsilon^2\lambda_2(\alpha,\beta) + \cdots. \tag{2.2b}$$

Here u_0, λ_0 satisfy (1.1). Substituting (2.2) into (2.1), and collecting terms of order ϵ, we obtain

$$\Delta u_1 + \lambda_0 F_u^0 u_1 = -\lambda_1 F^0, \quad x \in D, \tag{2.3a}$$

$$\partial_\nu u_1 + b u_1 = b h(s), \quad x \in \partial D, \tag{2.3b}$$

$$\int_D u_0 u_1\, dx = 0. \tag{2.3c}$$

Similarly, equating coefficients of ϵ^2 gives the following problem for u_2:

$$\Delta u_2 + \lambda_0 F_u^0 u_2 = -\lambda_2 F^0 - \lambda_1 F_u^0 u_1 - \frac{\lambda_0}{2} F_{uu}^0 u_1^2, \quad x \in D, \tag{2.4a}$$

$$\partial_\nu u_2 + b u_2 = 0, \quad x \in \partial D, \tag{2.4b}$$

$$\int_D (2u_0 u_2 + u_1^2)\, dx = 0. \tag{2.4c}$$

Here we have defined $F^0 \equiv F(u_0,\beta)$, $F_u^0 \equiv F_u(u_0,\beta)$, etc. The conditions (2.3c) and (2.4c) determine λ_1 and λ_2 uniquely away from points where the homogeneous version of (2.3a,b) has a non-trivial solution. At simple or cubic fold points the conditions (2.3c), (2.4c) serve only to specify the corrections u_i uniquely, and the λ_i are found by imposing solvability conditions on (2.3a,b), (2.4a,b).

The cubic fold point parameters for the perturbed problem (2.1) are denoted by $\alpha_c(\epsilon)$, $\beta_c(\epsilon)$, and $\lambda_c(\epsilon) \equiv \lambda\big(\alpha_c(\epsilon), \beta_c(\epsilon), \epsilon\big)$. We assume that $\alpha_c(\epsilon)$ and $\beta_c(\epsilon)$ can be expanded as

$$\alpha_c(\epsilon) = \alpha_0 + \epsilon\alpha_1 + \epsilon^2\alpha_2 + \cdots, \quad \beta_c(\epsilon) = \beta_0 + \epsilon\beta_1 + \epsilon^2\beta_2 + \cdots. \tag{2.5}$$

The equations for α_i and β_i are found from the requirement that

$$\lambda_\alpha\big(\alpha_c(\epsilon), \beta_c(\epsilon), \epsilon\big) = 0, \quad \lambda_{\alpha\alpha}\big(\alpha_c(\epsilon), \beta_c(\epsilon), \epsilon\big) = 0. \tag{2.6}$$

Substituting (2.5), (2.2b) in (2.6), and expanding for $\epsilon \ll 1$, we then set the coefficients of ϵ and ϵ^2 to zero to obtain the following equations for α_1, β_1, and β_2:

$$\beta_1 = -\frac{\lambda_{1\alpha}}{\lambda_{0\alpha\beta}}, \quad \alpha_1 = -\beta_1 \frac{\lambda_{0\alpha\alpha\beta}}{\lambda_{0\alpha\alpha\alpha}} - \frac{\lambda_{1\alpha\alpha}}{\lambda_{0\alpha\alpha\alpha}}, \tag{2.7a}$$

$$\begin{aligned}\beta_2 \lambda_{0\alpha\beta} = {} & -\lambda_{2\alpha} - \frac{\alpha_1^2}{2}\lambda_{0\alpha\alpha\alpha} - \frac{\beta_1^2}{2}\lambda_{0\alpha\beta\beta} \\ & - \alpha_1\beta_1\lambda_{0\alpha\alpha\beta} - \alpha_1\lambda_{1\alpha\alpha} - \beta_1\lambda_{1\alpha\beta}.\end{aligned} \tag{2.7b}$$

Here we have used the conditions $\lambda_{0\alpha}(\alpha_0, \beta_0) = 0$ and $\lambda_{0\alpha\alpha}(\alpha_0, \beta_0) = 0$, which characterizes the unperturbed cubic fold point. In terms of α_1, β_1, and β_2 the expansion of $\lambda_c(\epsilon)$ is given by

$$\lambda_c(\epsilon) = \lambda_{c0} + \epsilon\lambda_{c1} + \epsilon^2\lambda_{c2} + \cdots, \tag{2.8}$$

where λ_{c1} and λ_{c2} are seen to be given by

$$\begin{aligned} \lambda_{c1} &= \lambda_1 + \beta_1\lambda_{0\beta}, \\ \lambda_{c2} &= \lambda_2 + \beta_1\lambda_{1\beta} + \alpha_1\lambda_{1\alpha} + \frac{\beta_1^2}{2}\lambda_{0\beta\beta} + \alpha_1\beta_1\lambda_{0\alpha\beta} + \beta_2\lambda_{0\beta}. \end{aligned} \tag{2.9}$$

All quantities in (2.7) and (2.9) are to be evaluated at α_0, β_0. We now determine expressions for β_1 and λ_{c1} in terms of u_0 and $h(s)$. To do so, we must evaluate λ_1, $\lambda_{1\alpha}$, $\lambda_{0\beta}$, and $\lambda_{0\alpha\beta}$ at α_0, β_0.

We first determine λ_1 and $\lambda_{1\alpha}$ at α_0, β_0. We begin by differentiating (1.1) with respect to α to obtain

$$\begin{aligned} \triangle u_{0\alpha} + \lambda_0 F_u^0 u_{0\alpha} &= -\lambda_{0\alpha}F^0, \quad x \in D, \\ \partial_\nu u_{0\alpha} + b u_{0\alpha} &= 0, \quad x \in \partial D. \end{aligned} \tag{2.10}$$

A further differentiation in α then yields

$$\begin{aligned} \triangle u_{0\alpha\alpha} + \lambda_0 F_u^0 u_{0\alpha\alpha} &= -2\lambda_{0\alpha}F_u^0 u_{0\alpha} - \lambda_0 F_{uu}^0 u_{0\alpha}^2 - \lambda_{0\alpha\alpha}F^0, \quad x \in D, \\ \partial_\nu u_{0\alpha\alpha} + b u_{0\alpha\alpha} &= 0, \quad x \in \partial D. \end{aligned} \tag{2.11}$$

To determine λ_1 at α_0, β_0, we apply Green's theorem to (2.10) and (2.3a,b) to obtain

$$\lambda_1(F^0, u_{0\alpha}) = \int_{\partial D} \partial_\nu u_{0\alpha} h(s)\, ds + \lambda_{0\alpha}(F^0, u_1). \tag{2.12}$$

Here we have defined $(f, g) \equiv \int_D fg\, dx$. Evaluating (2.12) at α_0, β_0, where $\lambda_{0\alpha} = 0$, we find

$$\lambda_1 = \int_{\partial D} \partial_\nu u_{0\alpha} h(s)\, ds / (F^0, u_{0\alpha}). \tag{2.13}$$

To determine $\lambda_{1\alpha}$ at α_0, β_0, we first differentiate (2.12) with respect to α. Evaluating the resulting identity at α_0, β_0, where $\lambda_{0\alpha} = \lambda_{0\alpha\alpha} = 0$, we obtain

$$\lambda_{1\alpha} = \left[\frac{\int_{\partial D} \partial_\nu u_{0\alpha} h(s)\, ds}{(F^0, u_{0\alpha})}\right]_\alpha. \tag{2.14}$$

Now we determine $\lambda_{0\beta}$ and $\lambda_{0\alpha\beta}$ at α_0, β_0. Differentiating (1.1) with respect to β yields

$$\begin{aligned} \triangle u_{0\beta} + \lambda_0 F_u^0 u_{0\beta} &= -\lambda_{0\beta}F^0 - \lambda_0 F_\beta^0, \quad x \in D, \\ \partial_\nu u_{0\beta} + b u_{0\beta} &= 0, \quad x \in \partial D. \end{aligned} \tag{2.15}$$

Applying Green's theorem to (2.10) and (2.15), we derive

$$\lambda_{0\beta}(F^0, u_{0\alpha}) = -\lambda_0(F_\beta^0, u_{0\alpha}) + \lambda_{0\alpha}(F^0, u_{0\beta}). \tag{2.16}$$

Then evaluating (2.16) at α_0, β_0 gives

$$\lambda_{0\beta} = -\lambda_0(F_\beta^0, u_{0\alpha})/(F^0, u_{0\alpha}). \tag{2.17}$$

To determine $\lambda_{0\alpha\beta}$ at α_0 β_0, we differentiate (2.16) with respect to α and evaluate the resulting identity at α_0, β_0 to find

$$\lambda_{0\alpha\beta} = \lambda_0 (F^0_\beta, u_{0\alpha}) \frac{(F^0, u_{0\alpha})_\alpha}{(F^0, u_{0\alpha})^2} - \lambda_0 \frac{(F^0_\beta, u_{0\alpha})_\alpha}{(F^0, u_{0\alpha})}. \tag{2.18}$$

Here we have defined $(u, v)_\alpha \equiv (u_\alpha, v) + (u, v_\alpha)$.

Now substituting (2.14) and (2.18) into the expression for β_1 given in (2.7a), we obtain

$$\beta_1 = \lambda_0^{-1} \frac{\left[(F^0, u_{0\alpha})_\alpha \int_{\partial D} \partial_\nu u_{0\alpha} h(s)\, ds - (F^0, u_{0\alpha}) \int_{\partial D} \partial_\nu u_{0\alpha\alpha} h(s)\, ds\right]}{\left[(F^0_\beta, u_{0\alpha})(F^0, u_{0\alpha})_\alpha - (F^0, u_{0\alpha})(F^0_\beta, u_{0\alpha})_\alpha\right]}. \tag{2.19}$$

Then using (2.13), (2.17), and (2.19) in (2.9), we determine λ_{c1} as

$$\lambda_{c1} = \frac{1}{(F^0, u_{0\alpha})} \left[\int_{\partial D} \partial_\nu u_{0\alpha} h(s)\, ds - \lambda_0 \beta_1 (F^0_\beta, u_{0\alpha}) \right]. \tag{2.20}$$

We summarize our results in the following statement.

Proposition 2.1. *For the perturbed problem* (2.1) *in a bounded domain* $D \subset R^m$, *where* $m = 2$ *or* $m = 3$, *two-term expansions for* $\lambda_c(\epsilon)$ *and* $\beta_c(\epsilon)$ *are given by*

$$\begin{aligned} \beta_c(\epsilon) &= \beta_0 + \epsilon \beta_1 + \cdots, \\ \lambda_c(\epsilon) &= \lambda_{c0} + \epsilon \lambda_{c1} + \cdots. \end{aligned} \tag{2.21}$$

Formulas for β_1 *and* λ_{c1} *are given in* (2.19) *and* (2.20), *which are to be evaluated at* α_0, β_0.

We now show how to calculate the first correction α_1, defined in (2.7a), to the L_2 norm. To do so we must evaluate $\lambda_{0\alpha\alpha\alpha}$, $\lambda_{0\alpha\alpha\beta}$, and $\lambda_{1\alpha\alpha}$ at α_0, β_0. To determine $\lambda_{0\alpha\alpha\alpha}$, we first differentiate (2.11) with respect to α. Then upon evaluating the resulting expressions at α_0, β_0, we find

$$\begin{aligned} \triangle u_{0\alpha\alpha\alpha} + \lambda_0 F^0_u u_{0\alpha\alpha\alpha} &= -3\lambda_0 F^0_{uu} u_{0\alpha} u_{0\alpha\alpha} \\ &\quad - \lambda_{0\alpha\alpha\alpha} F^0 - \lambda_0 F^0_{uuu} u^3_{0\alpha}, \quad x \in D, \\ \partial_\nu u_{0\alpha\alpha\alpha} + b u_{0\alpha\alpha\alpha} &= 0, \quad x \in \partial D. \end{aligned} \tag{2.22}$$

Now applying Green's theorem to (2.10) and (2.22) at α_0, β_0, we obtain

$$\lambda_{0\alpha\alpha\alpha}(F^0, u_{0\alpha}) = -3\lambda_0 (F^0_{uu} u_{0\alpha\alpha}, u^2_{0\alpha}) - \lambda_0 (F^0_{uuu}, u^4_{0\alpha}). \tag{2.23}$$

In a similar way, we can determine $\lambda_{0\alpha\alpha\beta}$ and $\lambda_{1\alpha\alpha}$ at α_0, β_0. Omitting the details of the calculation, we find

$$\begin{aligned} \lambda_{0\alpha\alpha\beta}(F^0, u_{0\alpha}) &= -3\lambda_{0\beta}(F^0_u u_{0\alpha\alpha}, u_{0\alpha}) - 3\lambda_0 (F^0_{uu} u_{0\beta}, u_{0\alpha\alpha} u_{0\alpha}) \\ &\quad - 3\lambda_0 (F^0_{u\beta} u_{0\alpha\alpha}, u_{0\alpha}) - 2\lambda_{0\alpha\beta}(F^0, u_{0\alpha})_\alpha \\ &\quad - \lambda_0 (F^0_{uuu} u_{0\beta}, u^3_{0\alpha}) - \lambda_0 (F^0_{uu\beta}, u^3_{0\alpha}), \end{aligned} \tag{2.24}$$

and

$$\begin{aligned} \lambda_{1\alpha\alpha}(F^0, u_{0\alpha}) &= -3\lambda_1 (F^0_u u_{0\alpha\alpha}, u_{0\alpha}) - 3\lambda_0 (F^0_{uu} u_{0\alpha\alpha}, u_1 u_{0\alpha}) \\ &\quad - 2\lambda_{1\alpha}(F^0, u_{0\alpha})_\alpha - \lambda_0 (F^0_{uuu} u_1, u^3_{0\alpha}). \end{aligned} \tag{2.25}$$

Substituting (2.19), (2.23), (2.24), and (2.25) into (2.7a) determines α_1 in terms of u_0, u_1, and $h(s)$. We note that, in contrast to α_1, both β_1 and λ_{c1} can be calculated without knowing u_1.

3. Small temperature variation: circular cylindrical or spherical reactor

We now let D be a ball domain of radius unity in R^m with $m = 2, 3$. We parameterize the temperature perturbation $h(s)$ as $h(\theta)$ when $m = 2$ and $h(\theta, \phi)$ when $m = 3$. Here θ and ϕ are the circumferential and the polar angle, respectively. Since u_0 is assumed to be radially symmetric, the result (2.21) can be simplified as follows.

Corollary 3.1. *Consider* (2.1) *when D is a ball domain of radius one in R^m with $m = 2$ or $m = 3$. Then from* (2.19), (2.20), *and* (2.21) *the expansions for $\beta_c(\epsilon)$ and $\lambda_c(\epsilon)$ become*

$$\beta_c(\epsilon) = \beta_0 + \epsilon\beta_1^*\bar{h} + \cdots ,$$
$$\beta_1^* = \lambda_0^{-1}\frac{[\langle F^0, u_{0\alpha}\rangle_\alpha u'_{0\alpha}(1) - \langle F^0, u_{0\alpha}\rangle u'_{0\alpha\alpha}(1)]}{(\langle F^0_\beta, u_{0\alpha}\rangle\langle F^0, u_{0\alpha}\rangle_\alpha - \langle F^0, u_{0\alpha}\rangle\langle F^0_\beta, u_{0\alpha}\rangle_\alpha)}, \tag{3.1a}$$

$$\lambda_c(\epsilon) = \lambda_{c0} + \epsilon\lambda_{c1}^*\bar{h} + \cdots ,$$
$$\lambda_{c1}^* = \frac{1}{\langle F^0, u_{0\alpha}\rangle}\left[u'_{0\alpha}(1) - \lambda_0\beta_1^*\langle F^0_\beta, u_{0\alpha}\rangle\right]. \tag{3.1b}$$

In (3.1a,b) *the primes denote derivatives with respect to r, the angle brackets $\langle u, v\rangle$ are defined by $\langle u, v\rangle \equiv \int_0^1 uvr^{m-1}\,dr$, and the average temperature perturbation $\bar{h}$ is given by*

$$\bar{h} = \frac{1}{2\pi}\int_0^{2\pi} h(\theta)\,d\theta, \quad (m = 2),$$
$$\bar{h} = \frac{1}{4\pi}\int_0^{2\pi}\int_0^{\pi} h(\theta, \phi)\sin\phi\,d\phi\,d\theta, \quad (m = 3). \tag{3.2}$$

To determine numerical values for β_1^* and λ_{c1}^*, we use the extended system obtained from (1.1), (2.10), and (2.11). For the ball domain, this system can be written in $0 < r < 1$ as

$$Lu_0 + \lambda_0 F^0 = 0, \tag{3.3a}$$
$$Lu_{0\alpha} + \lambda_0 F^0_u u_{0\alpha} = -\lambda_{0\alpha}F^0, \tag{3.3b}$$
$$Lu_{0\alpha\alpha} + \lambda_0 F^0_u u_{0\alpha\alpha} = -2\lambda_{0\alpha}F^0_u u_{0\alpha} - \lambda_0 F^0_{uu}u^2_{0\alpha} - \lambda_{0\alpha\alpha}F^0. \tag{3.3c}$$

Here the operator L is defined by $Lu = r^{1-m}(r^{m-1}u')'$. The boundary conditions for (3.3) are

$$u'_0(1) + bu_0(1) = 0, \quad u'_{0\alpha}(1) + bu_{0\alpha}(1) = 0, \quad u'_{0\alpha\alpha}(1) + bu_{0\alpha\alpha}(1) = 0,$$
$$u'_0(0) = u'_{0\alpha}(0) = u'_{0\alpha\alpha}(0) = 0. \tag{3.4}$$

To complete the formulation of the extended system, we adjoin to (3.3)–(3.4) the defining relation (1.1c) for α. For this geometry, (1.1c) becomes $\alpha = 2^{m-1}\pi\int_0^1 u_0^2 r^{m-1}\,dr$, for $m = 2$ or $m = 3$. This system then is solved numerically using the collocation

b	λ_{c0}	β_0	λ^*_{c1}	β^*_1
∞	3.0063	.2421	-1.5507	-.0586
10.0	2.4822	.2428	-1.2768	-.0590
5.0	2.0867	.2443	-1.0674	-.0597
3.0	1.7014	.2460	-0.8644	-.0605
1.0	0.8504	.2491	-0.4268	-.0620
0.50	0.4786	.2497	-0.2396	-.0624
0.25	0.2544	.2499	-0.1272	-.0625

TABLE 1a. Temperature perturbation: $\lambda_{c0}, \beta_0, \lambda^*_{c1}$, β^*_1 for a circular cylindrical domain at different Biot numbers.

b	λ_{c0}	β_0	λ^*_{c1}	β^*_1
∞	5.0411	0.2388	-2.6335	-.0570
10.0	4.1466	0.2400	-2.1560	-.0576
5.0	3.4555	0.2425	-1.7798	-.0588
3.0	2.7781	0.2452	-1.4158	-.0601
1.0	1.3308	0.2491	-0.6678	-.0620
0.50	0.7347	0.2498	-0.3677	-.0624
0.25	0.3862	0.2499	-0.1931	-.0625

TABLE 1b. Temperature perturbation: λ_{c0}, β_0, λ^*_{c1}, β^*_1 for a spherical domain at different Biot numbers.

package COLSYS (see [2]). Since the solution is parameterized by α rather than λ_0, no sophisticated methods to compute past fold points are needed.

Numerical computations for $F(u,\beta) = \exp[u/(1+\beta u)]$. For a spherical domain, plots of α versus λ_0 for various values of β, with β near β_0 and with $b = \infty$, are shown in Figure 1. From this figure, we note that as β approaches β_0, the two simple fold points coalesce into a higher-order fold point. A similar situation occurs for a circular cylindrical domain.

To determine the unperturbed cubic fold point parameters α_0, β_0, and λ_{c0}, we solve (3.3), (3.4) subject to the side conditions $\lambda_{0\alpha} = \lambda_{0\alpha\alpha} = 0$. A Newton iteration scheme is used to enforce these conditions. To determine numerical values for the correction terms β^*_1 and λ^*_{c1}, defined in (3.1), the inner product integrals appearing there are evaluated at α_0, β_0 using a simple quadrature rule. In Table 1a, we give numerical values for β_0, λ_{c0}, β^*_1, and λ^*_{c1} at various Biot numbers b when $m = 2$. In Table 1b we give corresponding results when $m = 3$. From these tables we conclude that β^*_1 is an increasing function of the Biot number whereas λ^*_{c1} is a decreasing function of the Biot number. The fact that both of these quantities are negative is reasonable on physical grounds.

The data in Tables 1a,b indicate that the ratio $\lambda^*_{c1}/\lambda_{c0}$ is roughly constant over a wide range of Biot number b. Therefore, we write the expansion for $\lambda_c(\epsilon)$ in the form

$$\lambda_c(\epsilon) = \lambda_{c0}[1 - \epsilon \bar{h} f_1 + \cdots], \quad \text{as } \epsilon \to 0. \tag{3.5}$$

Numerical evidence suggests that the function f_1, which depends on b and on m, satisfies the following inequalities over the range $.25 < b < \infty$:

$$\begin{aligned} .5000 < f_1(b) < .5158, \quad (m = 2), \\ .5000 < f_1(b) < .5224, \quad (m = 3). \end{aligned} \tag{3.6}$$

It will be shown below that $f_1(b) \to 1/2$ as $b \to 0$ for $m = 2$ and $m = 3$. This suggests that (3.6) holds for the entire range $0 < b < \infty$. As for β, it is well-known (cf. [4]) that $\beta_0 \to 1/4$ as $b \to 0$ for $m = 2, 3$. We now show that $\beta_1^* \to -1/16$ as $b \to 0$ for $m = 2, 3$.

When $b \to 0$, the solutions u_0 and λ_0 to (1.1) can be parameterized as

$$u_0 = A + O(b), \quad \lambda_0 = \frac{mbA}{F(A,\beta)} + o(b), \quad \text{where} \quad A = \left(\frac{m\alpha}{\omega_m}\right)^{1/2}. \tag{3.7}$$

Here $\omega_2 \equiv 2\pi$ and $\omega_3 \equiv 4\pi$. The cubic fold point occurs where $\lambda_{0\alpha} = \lambda_{0\alpha\alpha} = 0$, which yields $\beta_0 \sim 1/4$, $\alpha_0 \sim 16\omega_m/m$, and $A_0 \sim 4$ as $b \to 0$. The value of λ_0 at this point satisfies $\lambda_{c0} \equiv \lambda_0(\alpha_0, \beta_0) \sim 4bm\exp(-2)$ as $b \to 0$. Using (3.7) in the defining relation (3.1) for λ_{c1}^* and β_1^*, we obtain that $f_1 \equiv -\lambda_{c1}^*/\lambda_{c0} \to 1/2$ and $\beta_1^* \to -1/16$ as $b \to 0$ for $m = 2, 3$. From the data in Tables 1a,b we observe that these asymptotic limits as $b \to 0$ are essentially achieved when $b = .25$.

3.1. Circular cylindrical domain: $\bar{h} = 0$. When $\bar{h} = 0$, both β_1 and λ_{c1} vanish. For this special case, we now determine the first non-vanishing corrections to β_0 and λ_{c0} for a circular cylindrical domain and a spherical domain.

In a circular cylindrical domain, the solution to (2.3) can be written as

$$u_1(r,\theta) = \frac{w_0(r)}{2} + \sum_{n=1}^{\infty} \big(w_n(r)\cos n\theta + v_n(r)\sin n\theta\big). \tag{3.8}$$

Substituting (3.8) into (2.3a), we obtain the following equations for w_n, v_n in $0 < r < 1$:

$$L_n w_n + \lambda_0 F_u^0 w_n = -2\lambda_1 F^0 \delta_{n0}, \quad (n \geq 0), \tag{3.9a}$$

$$L_n v_n + \lambda_0 F_u^0 v_n = 0, \quad (n \geq 1). \tag{3.9b}$$

Upon differentiating (3.9) with respect to α and evaluating the resulting expressions at α_0, β_0, we find

$$\begin{aligned} L_n w_{n\alpha} + \lambda_0 F_u^0 w_{n\alpha} &= -\lambda_0 F_{uu}^0 u_{0\alpha} w_n \\ &\quad - 2\lambda_{1\alpha} F^0 \delta_{n0} - 2\lambda_1 F_u^0 u_{0\alpha} \delta_{n0}, \quad (n \geq 0), \end{aligned} \tag{3.9c}$$

$$L_n v_{n\alpha} + \lambda_0 F_u^0 v_{n\alpha} = -\lambda_0 F_{uu}^0 u_{0\alpha} v_n, \quad (n \geq 1). \tag{3.9d}$$

The boundary conditions for (3.9) are

$$w_n'(1) + bw_n(1) = bc_n, \; w_{n\alpha}'(1) + bw_{n\alpha}(1) = 0, \quad (n \geq 0), \tag{3.10a}$$

$$v_n'(1) + bv_n(1) = b\,d_n, \; v_{n\alpha}'(1) + b\,v_{n\alpha}(1) = 0, \quad (n \geq 1). \tag{3.10b}$$

Here the operator L_n is defined by $L_n v \equiv r^{-1}(rv_r)_r - r^{-2}n^2 v$, and the constants c_n, d_n are the Fourier coefficients of $h(\theta)$, given by

$$\begin{aligned} c_n &= \frac{1}{\pi}\int_0^{2\pi} h(\theta)\cos n\theta\, d\theta, \quad (n \geq 0), \\ d_n &= \frac{1}{\pi}\int_0^{2\pi} h(\theta)\sin n\theta\, d\theta, \quad (n \geq 1). \end{aligned} \tag{3.11}$$

When $\bar{h} = c_0 = 0$, we find from (2.13) and (2.14) that $\lambda_1 = \lambda_{1\alpha} = 0$ at α_0, β_0. Since $\lambda_1 = 0$, the solution w_0 to (3.9a) at α_0, β_0 is an arbitrary multiple of $u_{0\alpha}$. Then the condition (2.3c) enforces that $w_0 = 0$. Thus, substituting (3.8) with $w_0 \equiv 0$ into (2.25), we obtain that $\lambda_{1\alpha\alpha} = 0$. Finally, from (2.7a) we conclude that $\alpha_1 = 0$ at α_0, β_0. Since $\beta_1 = \alpha_1 = \lambda_{c1} = 0$ at α_0, β_0, we must proceed further to obtain the first non-vanishing correction to the unperturbed cubic fold point values.

Since $\beta_1 = \alpha_1 = 0$, we note from (2.5), (2.7b), (2.8), and (2.9) that the second-order corrections β_2 and λ_{c2} can be evaluated after determining λ_2 and $\lambda_{2\alpha}$ at α_0, β_0. To determine λ_2, we apply Green's theorem to (2.4a,b) and (2.10) to obtain

$$\lambda_2(F^0, u_{0\alpha}) = -\lambda_1(F_u^0 u_1, u_{0\alpha}) - \frac{\lambda_0}{2}(F_{uu}^0 u_1^2, u_{0\alpha}) + \lambda_{0\alpha}(F^0, u_2). \tag{3.12}$$

Setting $\lambda_1 = 0$ in (3.12), and evaluating (3.12) at α_0, β_0, determines λ_2 as

$$\lambda_2(F^0, u_{0\alpha}) = -\frac{\lambda_0}{2}(F_{uu}^0 u_1^2, u_{0\alpha}). \tag{3.13}$$

To determine $\lambda_{2\alpha}$, we first differentiate (3.12) with respect to α. Then, evaluating the resulting expression at α_0, β_0 where $\lambda_{0\alpha} = \lambda_{0\alpha\alpha} = \lambda_1 = \lambda_{1\alpha} = 0$, we find

$$\begin{aligned} \lambda_{2\alpha}(F^0, u_{0\alpha}) = &-\lambda_2(F^0, u_{0\alpha})_\alpha - \lambda_0(F_{uu}^0 u_1 u_{1\alpha}, u_{0\alpha}) \\ &- \frac{\lambda_0}{2}(F_{uuu}^0 u_{0\alpha}^2 + F_{uu}^0 u_{0\alpha\alpha}, u_1^2). \end{aligned} \tag{3.14}$$

Finally, substituting the form (3.8) for u_1 into (3.13) and (3.14), and setting $w_0 = 0$, we obtain

$$\lambda_2\langle F^0, u_{0\alpha}\rangle = -\frac{\lambda_0}{4}\sum_{n=1}^{\infty}\langle F_{uu}^0 u_{0\alpha}, w_n^2 + v_n^2\rangle, \tag{3.15a}$$

$$\begin{aligned} \lambda_{2\alpha}\langle F^0, u_{0\alpha}\rangle = &-\lambda_2\langle F^0, u_{0\alpha}\rangle_\alpha - \frac{\lambda_0}{2}\sum_{n=1}^{\infty}\langle F_{uu}^0 u_{0\alpha}, w_n w_{n\alpha} + v_n v_{n\alpha}\rangle \\ &- \frac{\lambda_0}{4}\sum_{n=1}^{\infty}\langle F_{uuu}^0 u_{0\alpha}^2 + F_{uu}^0 u_{0\alpha\alpha}, w_n^2 + v_n^2\rangle. \end{aligned} \tag{3.15b}$$

Using (3.15) in (2.7b) and (2.9) determines β_2 and λ_{c2}. We summarize our results for this special case in the following statement.

Corollary 3.2. *Consider* (2.1) *when D is a circular cylindrical domain of radius one and assume that $\bar{h} = 0$. Then the expansions of $\lambda_c(\epsilon)$, $\beta_c(\epsilon)$ are given by*

$$\beta_c(\epsilon) = \beta_0 + \epsilon^2\beta_2 + \cdots, \quad \beta_2 = -\lambda_{2\alpha}/\lambda_{0\alpha\beta}, \tag{3.16a}$$

$$\lambda_c(\epsilon) = \lambda_{c0} + \epsilon^2\lambda_{c2} + \cdots, \quad \lambda_{c2} = \lambda_2 + \beta_2\lambda_{0\beta}. \tag{3.16b}$$

b	$n=1$	$n=2$	$n=3$	$n=4$	$n=5$
∞	-.395E-1	-.149E-1	-.827E-2	-.535E-2	-.376E-2
10.0	-.304E-1	-.108E-1	-.571E-2	-.351E-2	-.236E-2
5.0	-.215E-1	-.699E-2	-.343E-2	-.200E-3	-.128E-2
3.0	-.130E-1	-.379E-2	-.173E-2	-.951E-3	-.584E-3
1.0	-.185E-2	-.405E-3	-.157E-3	-.777E-4	-.442E-4
0.50	-.343E-3	-.665E-4	-.241E-4	-.114E-4	-.632E-5
0.25	-.529E-4	-.955E-5	-.333E-5	-.154E-5	-.837E-6

TABLE 2a. Temperature perturbation: λ_{c2} for a circular cylindrical domain with $h(\theta) = \cos(n\theta)$.

b	$n=1$	$n=2$	$n=3$	$n=4$	$n=5$
∞	-.225E-2	-.766E-3	-.401E-3	-.249E-3	-.170E-3
10.0	-.216E-2	-.704E-3	-.354E-3	-.211E-3	-.139E-3
5.0	-.191E-2	-.580E-3	-.275E-3	-.156E-3	-.983E-4
3.0	-.152E-2	-.418E-3	-.185E-3	-.100E-3	-.608E-4
1.0	-.494E-3	-.105E-3	-.402E-4	-.197E-4	-.111E-4
0.50	-.171E-3	-.326E-4	-.117E-4	-.551E-5	-.304E-5
0.25	-.509E-4	-.909E-5	-.315E-5	-.145E-5	-.787E-6

TABLE 2b. Temperature perturbation: β_2 for a circular cylindrical domain with $h(\theta) = \cos(n\theta)$.

Here $\lambda_{0\beta}$, $\lambda_{0\alpha\beta}$, λ_2, *and* $\lambda_{2\alpha}$ *are given in* (2.17), (2.18), (3.15a) *and* (3.15b), *respectively.*

Numerical Computations for $F(u,\beta) = \exp[u/(1+\beta u)]$. We now determine numerical values for β_2 and λ_{c2} in the special case when $h(\theta) = c_n \cos(n\theta)$ where n is a positive integer. Using the numerical solution to the extended system (3.3)–(3.4), we solve (3.9)–(3.10) using COLSYS to obtain w_n and $w_{n\alpha}$ at α_0, β_0, for various integers n. Then to determine β_2 and λ_{c2} defined in (3.16), the inner product integrals appearing in (3.15a,b) are evaluated by a numerical quadrature. Setting $c_n = 1$, in Tables 2a and 2b we give numerical values for λ_{c2} and β_2, respectively, for various Biot numbers and integers n. If $c_n \neq 1$, the entries in these tables should be multiplied by c_n^2. From Table 2a we observe that λ_{c2} is a decreasing function of b for fixed n and is an increasing function of n for fixed b. A similar qualitative dependence of β_2 on n and on b is observed from Table 2b. The data in Table 1a and Tables 2a,b can be combined to write explicit two-term expansions for $\lambda_c(\epsilon)$ and $\beta_c(\epsilon)$ for the values of b and n shown.

3.2. Spherical domain: $\bar{h} = 0$. In a spherical domain, (2.3) has a solution of the form

$$u_1(r,\theta,\phi) = \sum_{l=0}^{\infty} \sum_{n=-l}^{l} p_{ln}(r) Y_{ln}(\phi,\theta), \tag{3.17}$$

where $Y_{ln}(\phi,\theta)$ are the usual spherical harmonics. The unknown functions $p_{ln}(r)$, which depend on α and β, are to be determined.

Substituting (3.17) into (2.3a,b), and using the fact that Y_{ln} are orthonormal, we find that p_{ln} satisfies

$$L_l p_{ln} + \lambda_0 F^0_u p_{ln} = -\sqrt{4\pi}\lambda_1 F^0 \delta_{l0}, \quad 0 < r < 1, \tag{3.18a}$$

$$p'_{ln}(1) + b p_{ln}(1) = b c_{ln}. \tag{3.18b}$$

In (3.18a), the operator L_l is defined by $L_l v \equiv r^{-2}(r^2 v')' - l(l+1)r^{-2}v$ and the primes denote derivatives with respect to r. The complex constants c_{ln} are the coefficients in the spherical harmonic expansion of $h(\theta,\phi)$ given by

$$c_{ln} = \int_0^{2\pi}\int_0^{\pi} Y^*_{ln}(\phi,\theta)h(\theta,\phi)\sin\phi \, d\phi \, d\theta, \quad (l \geq 0, \ |n| \leq l). \tag{3.19}$$

Here the $*$ denotes complex conjugation. To determine the equation satisfied by $p_{ln\alpha}$, we differentiate (3.18) with respect to α, which yields the following problem for $0 \leq r \leq 1$:

$$L_l p_{ln\alpha} + \lambda_0 F^0_u p_{ln\alpha} = -\lambda_0 F^0_{uu} u_{0\alpha} p_{ln} - \lambda_{0\alpha} F^0_u p_{ln}$$
$$- \sqrt{4\pi}(\lambda_1 F^0_u u_{0\alpha} + \lambda_{1\alpha} F^0)\delta_{l0}, \tag{3.20a}$$

$$p'_{ln\alpha}(1) + b p_{ln\alpha}(1) = 0. \tag{3.20b}$$

Since h, and hence u_1, are real-valued functions, then $c_{ln} = (-1)^n c^*_{l-n}$ and $p_{ln}(r) = (-1)^n p^*_{l-n}(r)$. Thus c_{l0} and $p_{l0}(r)$ are real quantities.

When $\bar{h} = 0$, then $c_{00} = 0$ and so it follows that $\lambda_1 = \lambda_{1\alpha} = \lambda_{1\alpha\alpha} = 0$ at α_0, β_0. The condition (2.3c) then enforces that $p_{00}(r) = p_{00\alpha}(r) = 0$ at α_0, β_0. When $\bar{h} = 0$ the expansions of the cubic fold point parameters $\beta_c(\epsilon)$ and $\lambda_c(\epsilon)$ are given in (3.16). The terms λ_2 and $\lambda_{2\alpha}$, evaluated at α_0, β_0, which appear in (3.16) are given in (3.13) and (3.14), respectively.

Let $\phi_l(r)$ denote the solution to (3.18a) for $l \geq 1$ which satisfies the boundary condition $\phi'_l(1) + b\phi_l(1) = b$. In terms of ϕ_l, we have that $p_{ln} = c_{ln}\phi_l$ and $p_{ln\alpha} = c_{ln}\phi_{l\alpha}$ at α_0, β_0. Then substituting (3.17) into (3.13) and (3.14), we obtain the following expressions for λ_2 and $\lambda_{2\alpha}$ at α_0, β_0:

$$\lambda_2 \langle F^0, u_{0\alpha}\rangle = -\frac{\lambda_0}{8\pi}\sum_{l=1}^{\infty} a_l \langle F^0_{uu} u_{0\alpha}, \phi_l^2\rangle,$$
$$\lambda_{2\alpha}\langle F^0, u_{0\alpha}\rangle = -\lambda_2 \langle F^0, u_{0\alpha}\rangle_\alpha \tag{3.21}$$
$$- \frac{\lambda_0}{8\pi}\sum_{l=1}^{\infty} a_l \left[\langle F^0_{uuu} u^2_{0\alpha} + F^0_{uu} u_{0\alpha\alpha}, \phi_l^2\rangle + 2\langle F^0_{uu} u_{0\alpha}, \phi_l \phi_{l\alpha}\rangle\right].$$

In (3.21), the coefficients a_l for $l \geq 1$ are defined by

$$a_l = c^2_{l0} + 2\sum_{n=1}^{l} |c_{ln}|^2, \quad l \geq 1. \tag{3.22}$$

With λ_2 and $\lambda_{2\alpha}$ defined by (3.21), Corollary 3.2 gives a two-term expansion for $\beta_c(\epsilon)$ and $\lambda_c(\epsilon)$ for the case of a spherical domain with $\bar{h} = 0$.

Numerical computations for $F(u, \beta) = \exp[u/(1+\beta u)]$**.** For an arbitrary temperature perturbation with zero mean, the coefficients a_l can be calculated from (3.19) and (3.22). Since λ_{c2} and β_2 in (3.16) depend linearly on the a_l, it suffices to compute these terms only for the special case where $a_{l'} = 1$ and $a_l = 0$ for $l \neq l'$. For this special case, numerical results for λ_{c2} and β_2 for various values of l' and Biot number b are given in Tables 3a and 3b, respectively. By multiplying the entries in these tables by appropriate constants and using the results in Table 1b, we can obtain numerical values for the coefficients in the two-term expansions for $\lambda_c(\epsilon)$ and $\beta_c(\epsilon)$ that correspond to an arbitrary temperature perturbation with zero mean.

b	$l=1$	$l=2$	$l=3$	$l=4$	$l=5$
∞	-.185E-1	-.672E-2	-.369E-2	-.238E-2	-.167E-2
10.0	-.141E-1	-.484E-2	-.253E-2	-.155E-2	-.104E-2
5.0	-.955E-2	-.299E-2	-.145E-2	-.842E-3	-.539E-3
3.0	-.537E-2	-.150E-2	-.677E-3	-.372E-3	-.229E-3
1.0	-.624E-3	-.136E-3	-.529E-4	-.263E-4	-.151E-4
0.50	-.107E-3	-.213E-4	-.785E-5	-.377E-5	-.210E-5
0.25	-.159E-4	-.299E-5	-.107E-5	-.503E-6	-.277E-6

TABLE 3a. Temperature perturbation: λ_{c2} for a spherical domain with $h(\theta, \phi) = Y_{l0}(\phi, \theta)$.

b	$l=1$	$l=2$	$l=3$	$l=4$	$l=5$
∞	-.605E-3	-.198E-3	-.102E-3	-.634E-4	-.433E-4
10.0	-.580E-3	-.183E-3	-.909E-4	-.541E-4	-.355E-4
5.0	-.508E-3	-.148E-3	-.697E-4	-.395E-4	-.249E-4
3.0	-.387E-3	-.103E-3	-.450E-4	-.243E-4	-.148E-4
1.0	-.109E-3	-.231E-4	-.885E-5	-.437E-5	-.249E-5
0.50	-.353E-4	-.691E-5	-.252E-5	-.120E-5	-.669E-6
0.25	-.101E-4	-.189E-5	-.673E-6	-.316E-6	-.173E-6

TABLE 3b. Temperature perturbation: β_2 for a spherical domain with $h(\theta, \phi) = Y_{l0}(\phi, \theta)$.

4. A nearly circular cylindrical reactor

The perturbed problem in the nearly circular cylindrical domain D_ϵ: $0 \leq r \leq 1+\epsilon h(\theta)$ is

$$\Delta u + \lambda F(u, \beta) = 0, \quad x \in D_\epsilon, \tag{4.1a}$$

$$\partial_\nu u + bu = 0, \quad x \in \partial D_\epsilon. \tag{4.1b}$$

Here (r, θ) are polar coordinates and $h(\theta)$ is a smooth 2π periodic function. In these coordinates, (4.1b) becomes

$$u_r - \frac{\epsilon h'}{(1+\epsilon h)^2} u_\theta + b\left(1 + \frac{\epsilon^2 (h')^2}{(1+\epsilon h)^2}\right)^{1/2} u = 0 \quad \text{on} \quad r = 1 + \epsilon h(\theta). \tag{4.1c}$$

We seek the solution to (4.1), in terms of a parameter α, in the form (2.2a,b). The definition of α which we shall use here is

$$\alpha = \int_{D_\epsilon} u^2 \, dx. \tag{4.2}$$

The leading term in (2.2a) is the radially symmetric solution $u_0(r)$ to (4.1) in the unperturbed circular cylindrical domain D_0. Here we have suppressed the dependence of u_0 on α and β.

Substituting (2.2a,b) into (4.1), (4.2) and collecting terms of $O(\epsilon)$, we find that u_1 satisfies

$$\triangle u_1 + \lambda_0 F_u^0 u_1 = -\lambda_1 F_u^0, \quad r < 1, \tag{4.3a}$$

$$u_{1r} + b u_1 = -bhu_{0r} - hu_{0rr}, \quad \text{on} \quad r = 1, \tag{4.3b}$$

$$\int_{D_0} u_0 u_1 \, dx = -\pi u_0^2(1)\bar{h}. \tag{4.3c}$$

From the $O(\epsilon^2)$ terms, we obtain the following problem for u_2:

$$\triangle u_2 + \lambda_0 F_u^0 u_2 = -\lambda_2 F^0 - \lambda_1 F_u^0 u_1 - \frac{\lambda_0}{2} F_{uu}^0 u_1^2, \quad r < 1, \tag{4.4a}$$

$$\begin{aligned} u_{2r} + bu_2 = T_2(\theta) \equiv & -hu_{1rr} - \frac{h^2}{2} u_{0rrr} + h' u_{1\theta} \\ & + \frac{(h')^2}{2} u_{0r} - bhu_{1r} - \frac{bh^2}{2} u_{0rr}, \quad \text{on } r = 1, \end{aligned} \tag{4.4b}$$

$$\begin{aligned} \int_{D_0} (u_1^2 + 2u_0 u_2) \, dx = & -2\pi u_0(1) u_{0r}(1) \overline{h^2} \\ & - \pi u_0^2(1) \overline{h^2} - 4\pi u_0(1) \overline{h u_1(1,\theta)}. \end{aligned} \tag{4.4c}$$

Here we have defined $\bar{h} \equiv (2\pi)^{-1} \int_0^{2\pi} h(\theta) \, d\theta$.

The expansions of the cubic fold point parameters $\beta_c(\epsilon)$ and $\lambda_c(\epsilon)$ are given in (2.5) and (2.8), respectively. The coefficients β_1 and λ_{c1} in these expansions are defined in (2.7a) and (2.9). We now determine β_1 and λ_{c1} in terms of u_0 and $h(\theta)$.

To determine λ_1 at α_0, β_0, we first apply Green's theorem to (2.10) and (4.3a,b), which yields

$$\lambda_1(F^0, u_{0\alpha}) = 2\pi u_{0\alpha}(1)[bu_{0r}(1) + u_{0rr}(1)]\bar{h} + \lambda_{0\alpha}(F^0, u_1). \tag{4.5}$$

Evaluating (4.5) at α_0, β_0, where $\lambda_{0\alpha} = 0$, gives

$$\lambda_1 \langle F^0, u_{0\alpha} \rangle = u_{0\alpha}(1)[bu_{0r}(1) + u_{0rr}(1)]\bar{h}. \tag{4.6}$$

To determine $\lambda_{1\alpha}$ we differentiate (4.5) with respect to α and evaluate the resulting expression at α_0, β_0 to obtain

$$\lambda_{1\alpha} = \bar{h} \left[\frac{\big(bu_{0r}(1) + u_{0rr}(1)\big) u_{0\alpha}(1)}{\langle F^0, u_{0\alpha} \rangle} \right]_\alpha. \tag{4.7}$$

Then from (2.7a) and (2.9) we can write β_1 and λ_{c1} as

$$\beta_1 = \beta_1^* \bar{h}, \quad \text{where} \quad \beta_1^* = -\lambda_{0\alpha\beta}^{-1} \left[\frac{\big(bu_{0r}(1) + u_{0rr}(1)\big) u_{0\alpha}(1)}{\langle F^0, u_{0\alpha} \rangle} \right]_\alpha, \tag{4.8a}$$

$$\lambda_{c1} = \lambda_{c1}^* \bar{h}, \quad \text{where} \quad \lambda_{c1}^* = u_{0\alpha}(1) \frac{\big(bu_{0r}(1) + u_{0rr}(1)\big)}{\langle F^0, u_{0\alpha} \rangle} + \beta_1^* \lambda_{0\beta}. \tag{4.8b}$$

Here $\lambda_{0\beta}$ and $\lambda_{0\alpha\beta}$ are given in (2.17) and (2.18). In a similar way, we can determine α_1 defined in (2.7a). We summarize our results so far in the following statement.

Proposition 4.1. *Consider* (4.1) *in the nearly circular domain* $0 < r < 1 + \epsilon h(\theta)$. *Then the expansions for* $\beta_c(\epsilon)$ *and* $\lambda_c(\epsilon)$ *are*

$$\beta_c(\epsilon) = \beta_0 + \epsilon \beta_1^* \bar{h} + \cdots, \quad \lambda_c(\epsilon) = \lambda_{c0} + \epsilon \lambda_{c1}^* \bar{h} + \cdots. \tag{4.9}$$

We now consider the case where $\bar{h} = 0$. When $\bar{h} = 0$, it follows from (4.6), (4.7), and (4.8) that $\lambda_1 = \lambda_{1\alpha} = \beta_1 = \lambda_{c1} = 0$. A simple calculation also shows that $\alpha_1 = 0$. Thus, we must proceed further to obtain the first non-vanishing corrections to the unperturbed cubic fold point parameters.

When $\bar{h} = 0$, the expansions of $\lambda_c(\epsilon)$ and $\beta_c(\epsilon)$ have the form given in (3.16a,b). To determine β_2 and λ_{c2}, at α_0, β_0, which are defined in (3.16), we must evaluate λ_2 and $\lambda_{2\alpha}$. To determine λ_2, we apply Green's identity to (4.4) and (2.10), which yields

$$\begin{aligned} \lambda_2 (F^0, u_{0\alpha}) = {} & -\lambda_1 (F_u^0 u_1, u_{0\alpha}) - \frac{\lambda_0}{2} (F_{uu}^0 u_1^2, u_{0\alpha}) \\ & + \lambda_{0\alpha} (F^0, u_2) - 2\pi u_{0\alpha}(1) \overline{T_2}. \end{aligned} \tag{4.10}$$

Evaluating (4.10) at α_0, β_0, and setting $\lambda_1 = 0$, we find

$$\lambda_2 (F^0, u_{0\alpha}) = -\frac{\lambda_0}{2} (F_{uu}^0 u_1^2, u_{0\alpha}) - 2\pi u_{0\alpha}(1) \overline{T_2}. \tag{4.11}$$

To determine $\lambda_{2\alpha}$, we first differentiate (4.10) with respect to α. Then evaluating the resulting expression at α_0, β_0, where $\lambda_1 = \lambda_{1\alpha} = \lambda_{0\alpha} = \lambda_{0\alpha\alpha} = 0$, we obtain

$$\begin{aligned} \lambda_{2\alpha} (F^0, u_{0\alpha}) = {} & -\lambda_2 (F^0, u_{0\alpha})_\alpha - \lambda_0 (F_{uu}^0 u_1 u_{1\alpha}, u_{0\alpha}) \\ & - \frac{\lambda_0}{2} ([F_{uu}^0 u_{0\alpha}]_\alpha, u_1^2) - 2\pi \big(u_{0\alpha}(1) \overline{T_2}\big)_\alpha. \end{aligned} \tag{4.12}$$

Using (4.11) and (4.12) in (3.16a,b) determines β_2 and λ_{c2}.

We now determine β_2 and λ_{c2} in the special case where $h(\theta) = c_n \cos(n\theta)$ for some positive integer n. In this case, the unique solution u_1 to (4.3) has the form $u_1(r, \theta) = c_n w_n(r) \cos(n\theta)$ where $w_n(r)$ satisfies

$$\begin{aligned} & L_n w_n + \lambda_0 F_u^0 w_n = 0, \quad 0 < r < 1, \\ & w_n'(1) + b w_n(1) = -b u_{0r}(1) - u_{0rr}(1). \end{aligned} \tag{4.13}$$

The operator L_n is defined following (3.10). By differentiating (4.13) with respect to α, we obtain the following equation for $w_{n\alpha}$ at α_0, β_0:

$$\begin{aligned} & L_n w_{n\alpha} + \lambda_0 F_u^0 w_{n\alpha} = -\lambda_0 F_{uu}^0 u_{0\alpha} w_n, \quad 0 < r < 1, \\ & w_{n\alpha}'(1) + b w_{n\alpha}(1) = -b u_{0\alpha r}(1) - u_{0\alpha rr}(1). \end{aligned} \tag{4.14}$$

Setting $u_1 = c_n w_n(r)\cos(n\theta)$ in (4.11) and (4.12), we obtain

$$\lambda_2 \langle F^0, u_{0\alpha}\rangle = -\frac{\lambda_0 c_n^2}{4}\langle F^0_{uu} u_{0\alpha}, w_n^2\rangle - u_{0\alpha}(1)\overline{T_2}, \tag{4.15}$$

and

$$\begin{aligned}\lambda_{2\alpha}\langle F^0, u_{0\alpha}\rangle = -\lambda_2\langle F^0, u_{0\alpha}\rangle_\alpha - \frac{\lambda_0 c_n^2}{2}\langle F^0_{uu} u_{0\alpha}, w_n w_{n\alpha}\rangle \\ - \left(u_{0\alpha}(1)\overline{T_2}\right)_\alpha - \frac{\lambda_0 c_n^2}{4}\langle F^0_{uuu} u_{0\alpha}^2 + F^0_{uu} u_{0\alpha\alpha}, w_n^2\rangle.\end{aligned} \tag{4.16}$$

Finally, using (4.13) and the definition of T_2 given in (4.4b), we find

$$\begin{aligned}\overline{T_2} = \frac{c_n^2}{2}[(1-b)w_n'(1) + \lambda_0 w_n(1) F^0_u|_{r=1}] \\ - \frac{c_n^2}{4}[u_{0rrr}(1) - n^2 u_{0r}(1) + b u_{0rr}(1)].\end{aligned} \tag{4.17}$$

A similar expression, which we omit, can be written for $\overline{T_2}_\alpha$. We summarize the results for this special case as in the following statement.

Corollary 4.1. *Consider* (4.1) *in the nearly circular domain* $0 < r < 1 + \epsilon c_n \cos(n\theta)$. *Then the expansions for* $\beta_c(\epsilon)$ *and* $\lambda_c(\epsilon)$ *are*

$$\beta_c(\epsilon) = \beta_0 + \epsilon^2 \beta_2 + \cdots, \quad \beta_2 = -\lambda_{2\alpha}/\lambda_{0\alpha\beta}, \tag{4.18a}$$

$$\lambda_c(\epsilon) = \lambda_{c0} + \epsilon^2 \lambda_{c2} + \cdots, \quad \lambda_{c2} = \lambda_2 + \beta_2 \lambda_{0\beta}. \tag{4.18b}$$

Here λ_2 *and* $\lambda_{2\alpha}$ *are given in* (4.15) *and* (4.16). *These expansions are not uniformly valid as* $n \to \infty$ *and they become invalid when* $\epsilon n = O(1)$.

Numerical computations for $F(u,\beta) = \exp[u/(1+\beta u)]$**.** To determine numerical values for λ_2 and $\lambda_{2\alpha}$ at α_0, β_0 for $n \geq 1$ we first compute the numerical solution to the extended system (3.3), (3.4) at α_0, β_0 using the method described following (3.4). Then COLSYS is used to solve (4.13) and (4.14) for w_n and $w_{n\alpha}$. Next, the inner product integrals in (4.15) and (4.16) are evaluated using a numerical quadrature and thus β_2 and λ_{c2}, defined in (4.18), are determined. For $c_n = 1$, in Table 4a we give numerical values for λ_{c2} for various Biot numbers and integers n. In Table 4b we give corresponding results for β_2. If $c_n \neq 1$, the entries in these tables should be multiplied by c_n^2. The data in Table 1a and Tables 4a,b can be combined to write explicit two-term expansions for $\lambda_c(\epsilon)$ and $\beta_c(\epsilon)$.

From Table 4a we observe that for fixed b, λ_{c2} is an increasing function of n while for fixed $n > 1$, λ_{c2} is an increasing function of b. For $n = 1$, λ_{c2} is a decreasing function of b. Similar trends were found in [13] for the case of a simple fold point. As a partial check on the numerical results for λ_{c2}, a similar calculation to that given following (3.6) shows that $\lambda_{c2} \sim -4b(1 - n^2/2)e^{-2}$ as $b \to 0$. When $b = .25$, this limiting result is in close agreement with the numerical results given in the last row of Table 4a.

From Table 4b we observe that for fixed b, β_2 is a decreasing function of n. As a function of b for fixed n, β_2 first decreases with increasing b, then it increases for a while until it eventually starts decreasing again when b is sufficiently large. This trend has been confirmed by evaluating β_2 for other Biot numbers than those shown

b	$n=1$	$n=2$	$n=3$	$n=4$	$n=5$
∞	-1.503	4.125	7.913	11.29	14.52
10.0	-1.128	2.509	4.898	7.054	9.185
5.0	-0.872	1.688	3.532	5.394	7.432
3.0	-0.649	1.139	2.654	4.377	6.408
1.0	-0.262	0.446	1.342	2.529	4.028
0.50	-0.134	0.242	0.789	1.536	2.489
0.25	-0.068	0.128	0.431	0.852	1.391

TABLE 4a. Boundary perturbation: λ_{c2} for a circular cylindrical domain with $h(\theta) = \cos(n\theta)$.

b	$n=1$	$n=2$	$n=3$	$n=4$	$n=5$
∞	-.741E-5	-.331E-2	-.145E-1	-.220E-1	-.271E-1
10.0	-.313E-3	-.242E-2	-.122E-1	-.200E-1	-.265E-1
5.0	-.731E-3	-.254E-2	-.125E-1	-.221E-1	-.318E-1
3.0	-.911E-3	-.327E-2	-.128E-1	-.229E-1	-.337E-1
1.0	-.389E-3	-.217E-2	-.597E-2	-.995E-2	-.143E-1
0.50	-.130E-3	-.855E-3	-.214E-2	-.347E-2	-.491E-2
0.25	-.367E-4	-.265E-3	-.636E-3	-.101E-2	-.142E-2

TABLE 4b. Boundary perturbation: β_2 for a circular cylindrical domain with $h(\theta) = \cos(n\theta)$.

in Table 4b. However, a qualitative explanation for this non-monotone behavior is lacking.

As a check on the numerical results for β_2, λ_{c2}, we note that in the special case when $n = 1$, the solutions to (4.13) and (4.14) are simply $w_1 = -u_{0r}$ and $w_{1\alpha} = -u_{0\alpha r}$. Then we can simplify (4.15) and (4.16) by using the following identity which holds at α_0, β_0:

$$\lambda_0\langle F^0_{uu}u_{0\alpha}, u^2_{0r}\rangle = \lambda_0[u_{0\alpha}(1)u_{0r}(1)F^0_u|_{r=1} - u_{0\alpha r}(1)F^0\,|_{r=1}]. \tag{4.19}$$

Setting $w_1 = -u_{0r}$ in (4.15)–(4.17), and using (4.19) and (3.3a), we obtain at α_0, β_0 that

$$\begin{aligned} \lambda_2 &= \frac{c_1^2}{4}\left[\frac{\left(u_{0rr}(1)u_{0\alpha}(1) - u_{0\alpha r}(1)u_{0r}(1)\right)}{\langle F^0, u_{0\alpha}\rangle}\right], \\ \lambda_{2\alpha} &= \frac{c_1^2}{4}\left[\frac{\left(u_{0rr}(1)u_{0\alpha}(1) - u_{0\alpha r}(1)u_{0r}(1)\right)}{\langle F^0, u_{0\alpha}\rangle}\right]_\alpha, \end{aligned} \tag{4.20}$$

when $n = 1$. Substituting (4.20) in (4.18), we can write β_2 and λ_{c2} as

$$\beta_2 = -\frac{c_1^2}{4\lambda_{0\alpha\beta}}\left[\frac{\left(u_{0rr}(1)u_{0\alpha}(1) - u_{0\alpha r}(1)u_{0r}(1)\right)}{\langle F^0, u_{0\alpha}\rangle}\right]_\alpha, \quad (n=1), \tag{4.21a}$$

$$\lambda_{c2} = \frac{c_1^2}{4\langle F^0, u_{0\alpha}\rangle}\left[u_{0rr}(1)u_{0\alpha}(1) - u_{0\alpha r}(1)u_{0r}(1)\right] + \beta_2\lambda_{0\beta}, \quad (n=1). \tag{4.21b}$$

Using the numerical solution to (3.3), (3.4) directly in (4.21), we recover the entries in Tables 4a,b corresponding to $n = 1$.

5. Interior domain perturbations

Consider the following perturbed problem resulting from removing a small hole D_ϵ from a bounded domain $D \subset R^m$:

$$\triangle u + \lambda F(u, \beta) = 0, \quad x \in D \setminus D_\epsilon, \tag{5.1a}$$

$$\partial_\nu u + bu = 0, \quad x \in \partial D, \tag{5.1b}$$

$$\epsilon \partial_\nu u + \kappa u = 0, \quad x \in \partial D_\epsilon, \tag{5.1c}$$

$$\alpha = \int_{D \setminus D_\epsilon} u^2 \, dx. \tag{5.1d}$$

In (5.1), $b > 0$ and $\kappa > 0$ are constants, ∂_ν is the derivative of u with respect to the outward normal to $D \setminus D_\epsilon$, and D_ϵ is a small subdomain of 'radius' $O(\epsilon)$ centered at a point x_0 in D. We assume that D_ϵ can be written in terms of a fixed domain D_1 as $D_\epsilon = \epsilon D_1$. Our goal is to determine the corrections to the unperturbed cubic fold point values β_0 and λ_{c0} as a result of removing a hole D_ϵ from D.

In contrast to the regular perturbation problems considered in §2–4, we note that (5.1) is a singularly perturbed problem. Thus, for $\epsilon \ll 1$, the solution u to (5.1) is constructed using singular perturbation methods. We represent u by two different expansions for $\epsilon \ll 1$, an 'inner' expansion for x near x_0 and an 'outer' expansion for x far from x_0.

We expand λ in terms of the unknown gauge functions $\nu_i(\epsilon)$ as

$$\lambda(\alpha, \beta, \epsilon) = \lambda_0(\alpha, \beta) + \nu_1(\epsilon)\lambda_1(\alpha, \beta) + \nu_2(\epsilon)\lambda_2(\alpha, \beta) + \cdots . \tag{5.2}$$

In the outer region, away from the hole, we expand the solution as

$$u(x, \alpha, \beta, \epsilon) = u_0(x, \alpha, \beta) + \nu_1(\epsilon)u_1(x, \alpha, \beta) + \nu_2(\epsilon)u_2(x, \alpha, \beta) + \cdots . \tag{5.3}$$

Substituting (5.2), (5.3) into (5.1a,b,d), and equating terms of order $\nu_1(\epsilon)$, we find

$$\triangle u_1 + \lambda_0 F_u^0 u_1 = -\lambda_1 F^0, \quad x \neq x_0, \tag{5.4a}$$

$$\partial_\nu u_1 + bu_1 = 0, \quad x \in \partial D, \tag{5.4b}$$

$$\int_D u_0 u_1 \, dx = 0. \tag{5.4c}$$

The condition (5.4c) follows from (5.1d) in two relevant cases: $\nu_1(\epsilon) \gg O(\epsilon^m)$ with $u(x) - u(x_0) = O(1)$ for x near x_0, and $\nu_1(\epsilon) = O(\epsilon^m)$ with $u(x) - u(x_0) = o(1)$ for x near x_0. As shown below, the first case occurs when $\kappa \neq 0$ in (5.1c) whereas the second case occurs when $\kappa = 0$. Since the behavior of u_1 as $x \to x_0$ is not yet known, the function u_1 is not completely specified. To determine the behavior of u_1 as $x \to x_0$, we must construct an inner expansion near D_ϵ.

In the inner region, we write $y = \epsilon^{-1}(x - x_0)$ and $v(y, \alpha, \beta, \epsilon) = u(x_0 + \epsilon y, \alpha, \beta, \epsilon)$. Then from (5.1a,c) we obtain

$$\triangle_y v + \epsilon^2 \lambda F(v, \beta) = 0, \quad y \notin D_1; \quad \partial_\nu v + \kappa v = 0, \quad y \in \partial D_1. \tag{5.5}$$

Here $\triangle_y$, ∂_ν denote derivatives with respect to y and D_1 is the domain D_ϵ in the y variable.

The inner expansion is written in terms of other unknown gauge functions $\mu_i(\epsilon)$ as

$$v(y,\alpha,\beta,\epsilon) = \mu_0(\epsilon)v_0(y,\alpha,\beta) + \mu_1(\epsilon)v_1(y,\alpha,\beta) + \mu_2(\epsilon)v_2(y,\alpha,\beta) + \cdots . \quad (5.6)$$

Substituting (5.2) and (5.6) into (5.5), and assuming that $\mu_0(\epsilon) \gg O(\epsilon^2)$, we find

$$\triangle_y v_0 = 0, \quad y \notin D_1; \quad \partial_\nu v_0 + \kappa v_0 = 0, \quad y \in \partial D_1. \quad (5.7)$$

Equations for the higher-order inner corrections can be obtained in a similar way.

The inner and outer expansions must be asymptotically equal in some overlap domain within which y is large and $x - x_0$ is small. Omitting the dependence of u and v on α and β, we write the matching condition as

$$\begin{aligned} &u_0(x) + \nu_1(\epsilon)u_1(x) + \nu_2(\epsilon)u_2(x) + \cdots \\ &\quad \sim \mu_0(\epsilon)v_0(y) + \mu_1(\epsilon)v_1(y) + \mu_2(\epsilon)v_2(y) + \cdots . \end{aligned} \quad (5.8)$$

To derive expressions for the coefficients in the asymptotic expansions of the cubic fold point parameters, we proceed as in §2. Retaining only the leading-order correction terms, we find

$$\beta_c(\epsilon) = \beta_0 + \nu_1(\epsilon)\beta_1 + \cdots, \quad \beta_1 \equiv -\lambda_{1\alpha}/\lambda_{0\alpha\beta}, \quad (5.9a)$$

$$\lambda_c(\epsilon) = \lambda_{c0} + \nu_1(\epsilon)\lambda_{c1} + \cdots, \quad \lambda_{c1} \equiv \lambda_1 + \beta_1\lambda_{0\beta}. \quad (5.9b)$$

Here $\lambda_{0\beta}$ and $\lambda_{0\alpha\beta}$ are given in (2.17) and (2.18). The coefficients λ_{c1} and β_1 in (5.9) are to be evaluated at α_0, β_0.

5.1. Two dimensions. We first consider the case when $\kappa = 0$. In this case, a solution to (5.7) is an arbitrary constant. By choosing $\mu_0(\epsilon) = 1$ and $v_0(y) = u_0(x_0)$, the leading terms on the left and right sides of (5.8) are matched. To calculate further terms in the inner region, we choose $\mu_1(\epsilon) = \epsilon$ and $\mu_2(\epsilon) = \epsilon^2$. Then upon substituting (5.6) into (5.5), we obtain

$$\triangle_y v_1 = 0, \quad y \notin D_1; \qquad \partial_\nu v_1 = 0, \quad y \in \partial D_1, \quad (5.10a)$$

$$\triangle_y v_2 = -\lambda_0 F\big(u_0(x_0),\beta\big), \quad y \notin D_1; \qquad \partial_\nu v_2 = 0, \quad y \in \partial D_1. \quad (5.10b)$$

By expanding $u_0(x_0 + \epsilon y)$ for $\epsilon \ll 1$ in the matching condition (5.8), we find that the far field behaviors of v_1 and v_2 are

$$v_1(y) \sim \partial_{x_i}u_0(x_0)y_i, \quad v_2(y) \sim \frac{1}{2}\partial_{x_i}\partial_{x_j}u_0(x_0)y_iy_j, \quad \text{as} \quad y \to \infty. \quad (5.11)$$

¿From [14], the solutions to (5.10), (5.11) have the following asymptotic forms as $y \to \infty$:

$$v_1(y) \sim \partial_{x_i}u_0(x_0)\left[y_i + \frac{P_{ij}y_j}{|y|^2} + \cdots\right], \quad \text{as } y \to \infty, \quad (5.12a)$$

$$v_2(y) \sim \frac{1}{2}\partial_{x_i}\partial_{x_j}u_0(x_0)y_iy_j + E\log|y| + \cdots, \quad \text{as } y \to \infty. \quad (5.12b)$$

Here E is defined by

$$E = \frac{\lambda_0 A_1}{2\pi}F[u_0(x_0),\beta], \quad (5.13)$$

where P_{ij} is the polarizability tensor of D_1 and A_1 is the area of D_1.

Using (5.12a,b) in the matching condition (5.8), we find $\nu_1(\epsilon) = \epsilon^2$ and that u_1 has the following singular behavior as $x \to x_0$:

$$u_1(x) \sim \partial_{x_i} u_0(x_0) \frac{P_{ij}(x_j - x_{0j})}{|x - x_0|^2} + E \log|x - x_0|. \tag{5.14}$$

To match the as yet unaccounted for term of order $O(\epsilon^2 \log \epsilon)$ in (5.8), we must insert the switchback term $E(\epsilon^2 \log \epsilon)$ into the inner expansion (see [10] for a general discussion of switchback terms).

We now determine λ_1 and $\lambda_{1\alpha}$ at α_0, β_0 from the solution to (5.4), (5.14). To determine λ_1, we apply Green's identity to (5.4) and (2.10) in the region $D \setminus D_\sigma$ where D_σ is a small circle of radius σ about x_0. Letting $\sigma \to 0$ then yields

$$\lambda_1(F^0, u_{0\alpha}) = -\lim_{\sigma \to 0} \int_{\partial D_\sigma} (u_{0\alpha} \partial_\nu u_1 - u_1 \partial_\nu u_{0\alpha})\, ds + \lambda_{0\alpha}(F^0, u_1). \tag{5.15a}$$

To determine $\lambda_{1\alpha}$, we differentiate (5.15a) with respect to α to obtain

$$\begin{aligned} \lambda_{1\alpha}(F^0, u_{0\alpha}) = -\lambda_1(F^0, u_{0\alpha})_\alpha &- \lim_{\sigma \to 0} \int_{\partial D_\sigma} (u_{0\alpha} \partial_\nu u_1 - u_1 \partial_\nu u_{0\alpha})_\alpha\, ds \\ &+ \lambda_{0\alpha\alpha}(F^0, u_1) + \lambda_{0\alpha}(F^0, u_1)_\alpha. \end{aligned} \tag{5.15b}$$

Substituting (5.14) into (5.15a,b), and evaluating the resulting identities at α_0, β_0, where $\lambda_{0\alpha} = \lambda_{0\alpha\alpha} = 0$, determines λ_1 and $\lambda_{1\alpha}$ as

$$\lambda_1(F^0, u_{0\alpha}) = 2\pi[E u_{0\alpha}(x_0) - \partial_{x_i} u_{0\alpha}(x_0) P_{ij} \partial_{x_j} u_0(x_0)], \tag{5.16a}$$

$$\begin{aligned} \lambda_{1\alpha}(F^0, u_{0\alpha}) &= -\lambda_1(F^0, u_{0\alpha})_\alpha \\ &\quad + 2\pi\big[\big(E u_{0\alpha}(x_0)\big)_\alpha - \big(\partial_{x_i} u_{0\alpha}(x_0) P_{ij} \partial_{x_j} u_0(x_0)\big)_\alpha\big]. \end{aligned} \tag{5.16b}$$

Setting $(\alpha, \beta) = (\alpha_0, \beta_0)$ in (5.16), we find from (5.9) that β_1 and λ_{c1} are given by

$$\beta_1 = -\frac{2\pi}{\lambda_{0\alpha\beta}} \left[\frac{E u_{0\alpha}(x_0) - \partial_{x_i} u_{0\alpha}(x_0) P_{ij} \partial_{x_j} u_0(x_0)}{(F^0, u_{0\alpha})} \right]_\alpha, \tag{5.17a}$$

$$\lambda_{c1} = 2\pi \frac{[E u_{0\alpha}(x_0) - \partial_{x_i} u_{0\alpha}(x_0) P_{ij} \partial_{x_j} u_0(x_0)]}{(F^0, u_{0\alpha})} + \beta_1 \lambda_{0\beta}. \tag{5.17b}$$

Here the constant E, defined in (5.13), is to be evaluated at α_0, β_0. Then substituting (5.17) in (5.9), we obtain a two-term expansion for $\beta_c(\epsilon)$ and $\lambda_c(\epsilon)$ which we summarize as follows.

Proposition 5.1. *For dimension $m = 2$, assume $\kappa = 0$ in* (5.1c). *Then*

$$\beta_c(\epsilon) = \beta_0 + \epsilon^2 \beta_1 + \cdots, \quad \lambda_c(\epsilon) = \lambda_{c0} + \epsilon^2 \lambda_{c1} + \cdots. \tag{5.18}$$

We now consider the case where $\kappa > 0$ in (5.1c). In this case, (5.7) has a solution $\hat{v}(y)$ with the asymptotic behavior

$$\hat{v}(y) = \log|y| - \log[d(\kappa)] + \cdots, \quad \text{as} \quad |y| \to \infty. \tag{5.19}$$

When $\kappa = \infty$, $d(\infty)$ is called the logarithmic capacitance of D_1. Using the matching condition (5.8), we obtain $\nu_1(\epsilon) = \mu_0(\epsilon) = -1/\log[\epsilon d(\kappa)]$, $v_0(y) = u_0(x_0)\hat{v}(y)$ and that u_1 has the following singular behavior as $x \to x_0$:

$$u_1(x) \sim u_0(x_0) \log|x - x_0|. \tag{5.20}$$

We now determine λ_1, $\lambda_{1\alpha}$ at α_0, β_0 from the solution u_1 to (5.4), (5.20). Substituting (5.20) into (5.15a,b) we obtain at α_0, β_0, that

$$\lambda_1(F^0, u_{0\alpha}) = 2\pi u_0(x_0)u_{0\alpha}(x_0), \tag{5.21a}$$

$$\lambda_{1\alpha}(F^0, u_{0\alpha}) = -\lambda_1(F^0, u_{0\alpha})_\alpha + 2\pi\left[u_{0\alpha\alpha}(x_0)u_0(x_0) + \left(u_{0\alpha}(x_0)\right)^2\right]. \tag{5.21b}$$

Using (5.21) in (5.9) determines β_1 and λ_{c1} at α_0, β_0 as

$$\beta_1 = -\frac{2\pi}{\lambda_{0\alpha\beta}}\left[\frac{u_0(x_0)u_{0\alpha}(x_0)}{(F^0, u_{0\alpha})}\right]_\alpha, \quad \lambda_{c1} = \frac{2\pi u_0(x_0)u_{0\alpha}(x_0)}{(F^0, u_{0\alpha})} + \beta_1\lambda_{0\beta}. \tag{5.22}$$

Then substituting (5.22) in (5.9) we obtain a two-term expansion for $\beta_c(\epsilon)$ and $\lambda_c(\epsilon)$ which we summarize as follows.

Proposition 5.2. *For dimension $m = 2$, assume $\kappa > 0$ in* (5.1c). *Then*

$$\begin{aligned} \beta_c(\epsilon) &= \beta_0 + \left(-\frac{1}{\log[\epsilon d(\kappa)]}\right)\beta_1 + \cdots, \\ \lambda_c(\epsilon) &= \lambda_{c0} + \left(-\frac{1}{\log[\epsilon d(\kappa)]}\right)\lambda_{c1} + \cdots. \end{aligned} \tag{5.23}$$

Both β_1 and λ_{c1}, determined by (5.22), *are to be evaluated at α_0, β_0.*

We note that we can simplify (5.23) when $\kappa = \epsilon\kappa_0$, where κ_0 is independent of ϵ. In the limit $\kappa \to 0$, we apply the divergence theorem to (5.7) and (5.19) to derive $\log[d(\kappa)] \sim -2\pi/L_1\kappa$, where L_1 is the length of ∂D_1. Then with $\kappa = \epsilon\kappa_0$, the leading-order corrections to the unperturbed cubic fold point parameters are found by replacing $\left(-1/\log[\epsilon d(\kappa)]\right)$ in (5.23) by $\epsilon L_1\kappa_0/2\pi$.

When F is sufficiently smooth and $\kappa > 0$, the result (5.23) can be extended to higher-order in powers of $\left(-1/\log[\epsilon d(\kappa)]\right)$. By following a similar procedure as in [15], where the case of a simple fold point was considered, it can be shown that the expansions of $\beta_c(\epsilon)$ and $\lambda_c(\epsilon)$ start with infinite series in powers of $\left(-1/\log[\epsilon d(\kappa)]\right)$. These expansions have the form

$$\begin{aligned} \lambda_c(\epsilon) &= \lambda_{c0} + \sum_{i=1}^{\infty}\left(-\frac{1}{\log[\epsilon d(\kappa)]}\right)^i \lambda_{ci} + \cdots, \\ \beta_c(\epsilon) &= \beta_0 + \sum_{i=1}^{\infty}\left(-\frac{1}{\log[\epsilon d(\kappa)]}\right)^i \beta_i, + \cdots, \end{aligned} \tag{5.24}$$

where the coefficients β_i and λ_{ci} are independent of ϵ, of κ, and of the shape of the hole D_1.

5.2. Three dimensions. We first treat the case where $\kappa = 0$ in (5.1c). This case is very similar to the corresponding case in two dimensions and so we omit most of the details. In the inner region, we expand the solution as $v = u_0(x_0) + \epsilon v_1 + \epsilon^2 v_2 + \cdots$, where v_1 and v_2 satisfy (5.10a,b), (5.11). From [14] the far field behaviors of v_1 and v_2, in analogy with (5.12a,b), are

$$v_1(y) \sim \partial_{x_i}u_0(x_0)\left[y_i + \frac{P_{ij}y_j}{|y|^3} + \cdots\right], \quad \text{as } y \to \infty, \tag{5.25a}$$

$$v_2(y) \sim \frac{1}{2}\partial_{x_i}\partial_{x_j}u_0(x_0)y_iy_j - \frac{E}{|y|} + \cdots, \quad \text{as } y \to \infty. \tag{5.25b}$$

The constant E is given in terms of the volume V_1 of D_1 by

$$E = \frac{\lambda_0 V_1}{4\pi} F[u_0(x_0), \beta]. \tag{5.26}$$

Using (5.25a,b) in the matching condition (5.8), we find $\nu_1(\epsilon) = \epsilon^3$ and we require that u_1 have the following singular behavior as $x \to x_0$:

$$u_1(x) \sim \partial_{x_i} u_0(x_0) \frac{P_{ij}(x_j - x_{0j})}{|x - x_0|^3} - \frac{E}{|x - x_0|}. \tag{5.27}$$

Using (5.27) in (5.15a,b), where D_σ is a small sphere of radius σ centered at x_0, we can calculate λ_1 and $\lambda_{1\alpha}$ at α_0, β_0. Then, in analogy with (5.17), we find at α_0, β_0 that

$$\beta_1 = -\frac{4\pi}{\lambda_{0\alpha\beta}} \left[\frac{E u_{0\alpha}(x_0) - \partial_{x_i} u_{0\alpha}(x_0) P_{ij} \partial_{x_j} u_0(x_0)}{(F^0, u_{0\alpha})} \right]_\alpha, \tag{5.28a}$$

$$\lambda_{c1} = 4\pi \frac{[E u_{0\alpha}(x_0) - \partial_{x_i} u_{0\alpha}(x_0) P_{ij} \partial_{x_j} u_0(x_0)]}{(F^0, u_{0\alpha})} + \beta_1 \lambda_{0\beta}. \tag{5.28b}$$

Here the constant E, defined in (5.26), is to be evaluated at α_0, β_0. Using (5.28) in (5.9), we obtain a two-term expansion for $\beta_c(\epsilon)$ and $\lambda_c(\epsilon)$ which we summarize as follows.

Proposition 5.3. *For dimension $m = 3$, assume $\kappa = 0$ in* (5.1c). *Then*

$$\beta_c(\epsilon) = \beta_0 + \epsilon^3 \beta_1 + \cdots, \quad \lambda_c(\epsilon) = \lambda_{c0} + \epsilon^3 \lambda_{c1} + \cdots. \tag{5.29}$$

We now consider the case where $\kappa > 0$ in (5.1c). In three dimensions, (5.7) has a solution $\hat{v}(y)$ with the asymptotic form

$$\hat{v}(y) = 1 - \frac{C(\kappa)}{|y|} + \cdots. \tag{5.30}$$

Here $C(\kappa)$ is a constant depending on κ and the shape of the domain D_1. When $\kappa = \infty$, $C(\infty)$ is the capacitance of D_1. Matching the terms in (5.8), we find that $\mu_0(\epsilon) = 1$, $v_0(y) = u_0(x_0)\hat{v}(y)$, and $\nu_1(\epsilon) = \epsilon$. Moreover, u_1 has the singular form

$$u_1(x) \sim -u_0(x_0) C(\kappa)/|x - x_0|, \quad \text{as } x \to x_0. \tag{5.31}$$

The problem for u_1 and λ_1 is given by (5.4) and (5.31).

We now determine λ_1 and $\lambda_{1\alpha}$ at α_0, β_0 from (5.15a,b), where D_σ is a small sphere of radius σ centered at x_0. Substituting (5.31) into (5.15a,b), we find at α_0, β_0 that

$$\lambda_1 = 4\pi C(\kappa) \frac{u_0(x_0) u_{0\alpha}(x_0)}{(F^0, u_{0\alpha})}, \quad \lambda_{1\alpha} = 4\pi C(\kappa) \left[\frac{u_0(x_0) u_{0\alpha}(x_0)}{(F^0, u_{0\alpha})} \right]_\alpha. \tag{5.32}$$

Using (5.32) in (5.9), we can write β_1 and λ_{c1} as $\beta_1 = C(\kappa)\beta_1^*$ and $\lambda_{c1} = C(\kappa)\lambda_{c1}^*$ where

$$\beta_1^* = -\frac{4\pi}{\lambda_{0\alpha\beta}} \left[\frac{u_0(x_0) u_{0\alpha}(x_0)}{(F^0, u_{0\alpha})} \right]_\alpha, \quad \lambda_{c1}^* = 4\pi \frac{u_0(x_0) u_{0\alpha}(x_0)}{(F^0, u_{0\alpha})} + \beta_1^* \lambda_{0\beta}. \tag{5.33}$$

Then substituting (5.33) in (5.9), we obtain a two-term expansion for $\beta_c(\epsilon)$ and $\lambda_c(\epsilon)$ which we summarize as follows.

Proposition 5.4. *For dimension $m = 3$, assume $\kappa > 0$ in* (5.1c). *Then*

$$\beta_c(\epsilon) = \beta_0 + \epsilon C(\kappa)\beta_1^* + \cdots, \quad \lambda_c(\epsilon) = \lambda_{c0} + \epsilon C(\kappa)\lambda_{c1}^* + \cdots. \tag{5.34}$$

The expansions in (5.34) can be simplified as $\kappa \to 0$ by using $C(\kappa) \sim S_1\kappa_0/4\pi$, where S_1 is the surface area of ∂D_1. Thus, if $\kappa = \epsilon\kappa_0$ with κ_0 independent of ϵ, the leading-order corrections to the cubic fold point parameters are found by replacing $\epsilon C(\kappa)$ in (5.34) with $\epsilon^2 S_1\kappa_0/4\pi$.

6. Comparison of asymptotic and numerical results for interior perturbations

We now show how to evaluate the coefficients in the asymptotic expansions of $\lambda_c(\epsilon)$ and $\beta_c(\epsilon)$, given in Propositions 5.1–5.4, for a circular cylindrical domain or a spherical domain, each of radius one, containing a small hole. The hole, which may be either cooling ($\kappa > 0$) or insulating ($\kappa = 0$), is located at a distance r_0 (with $0 \le r_0 < 1$) from the origin.

The coefficients in the expansions for $\lambda_c(\epsilon)$ and $\beta_c(\epsilon)$ depend on quantities associated with the unperturbed solution at α_0, β_0. We consider unperturbed solutions u_0 that are radially symmetric in the circular cylindrical or spherical geometry. Thus, in Propositions 5.1–5.4 we replace $u_0(x)$ by $u_0(r)$ and $u_0(x_0)$ by $u_0(r_0)$. Here $u_0(r)$ is computed numerically from (3.3)–(3.4). The asymptotic results also depend on various constants that are associated with the hole geometry and the boundary condition for u on the hole. In the two-dimensional case, we must determine $d(\kappa)$ and the tensor P_{ij}, defined from (5.7), (5.19) and (5.10a), (5.12a), respectively. If D_1 is a circle of radius a, then $d(\kappa) = a\exp[-1/\kappa a]$ and $P_{ij} = a^2\delta_{ij}$. If D_1 is an ellipse with semi-axes a and a^{-1}, then $d(\infty) = (a + a^{-1})/2$. Numerical values for $d(\kappa)$ for other hole shapes were computed previously in [15] and the results are summarized in Appendix A. In the three-dimensional case, we must determine $C(\kappa)$, defined from (5.7), (5.30), and the tensor P_{ij}, defined from (5.10a), (5.25a). If D_1 is a sphere of radius a, then $C(\kappa) = a\kappa/(1 + a\kappa)$ and $P_{ij} = a^3\delta_{ij}/2$. The capacitance $C(\infty)$ also is known explicitly when D_1 is an ellipsoid.

In the limiting cases of concentric circular cylinders or concentric spheres, the asymptotic results for $\lambda_c(\epsilon)$ and $\beta_c(\epsilon)$ will be compared with corresponding numerical results obtained from the full problem (5.1). In both cases, the inner radius is taken to be ϵ. For these geometries, the cubic fold point parameters $\lambda_c(\epsilon)$ and $\beta_c(\epsilon)$ for the full perturbed problem are determined from the numerical solution to

$$\begin{gathered} u'' + \frac{(m-1)}{r}u' + \lambda F(u, \beta) = 0, \quad \epsilon \le r \le 1, \\ u'(1) + bu(1) = 0, \quad \epsilon u'(\epsilon) - \kappa u(\epsilon) = 0, \quad \alpha = 2^{m-1}\pi\int_\epsilon^1 u^2 r^{m-1}\, dr. \end{gathered} \tag{6.1}$$

To locate the cubic fold point for (6.1), we proceed by writing the extended system for (6.1) in analogy with (3.3). This system is solved numerically using COLSYS with care taken to resolve the boundary layer near $r = \epsilon$. For fixed ϵ, the cubic fold point parameters $\lambda_c(\epsilon)$ and $\beta_c(\epsilon)$ are determined by appending the side conditions $\lambda_\alpha = \lambda_{\alpha\alpha} = 0$ to the extended system. Then using a simple continuation in ϵ the curves $\lambda_c(\epsilon)$ and $\beta_c(\epsilon)$ are obtained. For illustration purposes, the computations below are done for the combustion form $F(u, \beta) = \exp[u/(1 + \beta u)]$. Similar results can be obtained for other nonlinearities associated with cubic fold point behavior.

r_0	$\lambda_{c1}(5.22)$	$\beta_1(5.22)$	$\lambda_{c1}(5.17b)$	$\beta_1(5.17a)$
.10	3.9043	0.1067×10^{-1}	10.883	0.0239
.30	3.0094	0.3865×10^{-2}	5.521	-0.0342
.50	1.7092	-0.1679×10^{-2}	-1.288	-0.0455
.70	0.6151	-0.1531×10^{-2}	-5.440	0.0154
.90	0.0636	-0.8865×10^{-4}	-6.331	0.0253

TABLE 5a. The coefficients λ_{c1} and β_{c1}, when $b = \infty$, for a cooling rod or insulating rod of circular cross-section located at a distance r_0 from the origin of a circular cylindrical domain.

b	$\lambda_{c1}(5.22)$	$\beta_1(5.22)$	$\lambda_{c1}(5.17b)$	$\beta_1(5.17a)$
∞	4.0299	0.01179	11.667	0.03485
10.0	3.3397	0.01207	7.9647	0.03075
5.0	2.8468	0.01208	5.6779	0.02759
3.0	2.4049	0.01104	3.8810	0.02176
1.0	1.6151	0.00543	1.2791	0.00586
0.50	1.3541	0.00277	0.6002	0.00175
0.25	1.2186	0.00136	0.2866	0.00047

TABLE 5b. The coefficients λ_{c1} and β_{c1} for a cooling rod or insulating rod of circular cross-section centered at the origin of a circular cylindrical domain.

6.1. Two dimensions: circular cylindrical domain. In the case of an insulating rod ($\kappa = 0$), the expansions of $\lambda_c(\epsilon)$ and $\beta_c(\epsilon)$ are given in Proposition 5.1, where the coefficients λ_{c1} and β_1 are given in (5.17). In order to evaluate these coefficients numerically, we will consider only insulating rods of circular cross-section and radius ϵ for which $P_{ij} = \delta_{ij}$. In the case of a cooling rod ($\kappa > 0$), the expansions of $\lambda_c(\epsilon)$ and $\beta_c(\epsilon)$ are given in Proposition 5.2, where the coefficients λ_{c1} and β_1 are given in (5.22). These coefficients are independent of κ and of the shape of the cross-section of the rod.

When $b = \infty$, in Table 5a we give numerical values for λ_{c1} and β_1 for a cooling rod and for an insulating rod of circular cross-section located at various distances r_0 from the origin. When $r_0 = 0$, in Table 5b we give numerical values, at various Biot numbers, for λ_{c1} and β_1 for cooling rods and for insulating rods of circular cross-section. By combining the results in Table 1a and Tables 5a,b, and by using the numerical values for $d(\kappa)$ given in Appendix A, the coefficients in the two-term expansions for $\lambda_c(\epsilon)$ and $\beta_c(\epsilon)$ are known for various κ, b, and hole shapes.

Suppose that an insulating rod of circular cross-section is centered at the origin. Then for $b = \infty$, in Table 6 we compare the two-term asymptotic result (5.18) for $\lambda_c(\epsilon)$ and $\beta_c(\epsilon)$ with corresponding numerical results obtained from the full problem (6.1). From this table we observe that the asymptotic results for $\lambda_c(\epsilon)$ and $\beta_c(\epsilon)$ are within 3% of the corresponding numerical results even when $\epsilon = .15$. Similar close agreement between the asymptotic and numerical results for $\lambda_c(\epsilon)$ and $\beta_c(\epsilon)$ is found for other Biot numbers b.

Now consider the case of a cooling rod of circular cross-section centered at the

ϵ	$\lambda_c(5.18)$	$\lambda_c(6.1)$	$\beta_c(5.18)$	$\beta_c(6.1)$
0.005	3.0066	3.0066	0.24210	0.24211
0.010	3.0075	3.0075	0.24210	0.24211
0.025	3.0136	3.0136	0.24212	0.24213
0.050	3.0355	3.0351	0.24219	0.24219
0.075	3.0719	3.0706	0.24230	0.24227
0.100	3.1230	3.1198	0.24245	0.24238
0.125	3.1886	3.1827	0.24264	0.24251
0.150	3.2688	3.2595	0.24288	0.24264

TABLE 6. Comparison of asymptotics and numerics for an insulating rod concentric with a circular cylindrical domain with $b = \infty$.

origin with $\kappa = \infty$. Then when $b = \infty$, a three-term expansion for $\lambda_c(\epsilon)$ and $\beta_c(\epsilon)$ was given previously in Lange and Weinitschke [11]. For this special geometry, they showed, using a different asymptotic method from that given in §5, that

$$\lambda_c(\epsilon) = 3.0063 + 4.0297\Big(-\frac{1}{\log \epsilon}\Big) + 4.4250\Big(-\frac{1}{\log \epsilon}\Big)^2 + \cdots, \tag{6.2a}$$

$$\beta_c(\epsilon) = 0.2421 + 0.0118\Big(-\frac{1}{\log \epsilon}\Big) - 0.0023\Big(-\frac{1}{\log \epsilon}\Big)^2 + \cdots. \tag{6.2b}$$

Note, from Table 5b, we have obtained the slightly different result $\lambda_{c1} = 4.0299$. This very minor discrepancy is probably a result of a small error, of unknown origin, in numerically computing λ_{c1}. By adapting the analysis in [15], where the case of a simple fold point was analyzed, it can be shown that the expansions of $\lambda_c(\epsilon)$ and $\beta_c(\epsilon)$ for a cooling rod of arbitrary cross-section, with $\kappa > 0$, start with infinite logarithmic series of the form given in (5.24). The coefficients λ_{ci} and β_i, for $i \geq 1$, in these series are independent of ϵ, of κ, and of the shape of the cross-section of the cooling rod. Therefore, by replacing ϵ by $\epsilon d(\kappa)$ in (6.2), the three-term results of [11] also apply when a cooling rod of arbitrary cross-section, with $\kappa > 0$, is centered at the origin. For this geometry, we now show how to obtain even further terms in the expansions of $\lambda_c(\epsilon)$ and $\beta_c(\epsilon)$.

6.2. Two dimensions: summing the logarithmic series. Suppose that a cooling rod of arbitrary cross-section, with $\kappa > 0$, is centered at the origin of a circular cylindrical domain. We now formulate a certain related problem whose solutions are asymptotic to the sum of the logarithmic series for $\lambda_c(\epsilon)$ and $\beta_c(\epsilon)$ written in (5.24). The method we use to sum these logarithmic series is very closely related to the method used in [15] to sum a similar series resulting from an expansion of a simple fold point.

We begin by defining $\lambda_c^*(z)$ and $\beta_c^*(z)$ as functions asymptotic to the sum of the terms written explicitly on the right side of (5.24), namely

$$\lambda_c^*(z) \sim \lambda_{c0} + \sum_{i=1}^{\infty}\Big(\frac{-1}{\log z}\Big)^i \lambda_{ci}, \quad \beta_c^*(z) \sim \beta_0 + \sum_{i=1}^{\infty}\Big(\frac{-1}{\log z}\Big)^i \beta_i. \tag{6.3}$$

Here the parameter z is defined by $z \equiv \epsilon d(\kappa)$. The key observation, derived by formally extending the analysis in §5 to infinite-order in powers of $-1/\log[\epsilon d(\kappa)]$, is that $\lambda_c^*(z)$ and $\beta_c^*(z)$ correspond to the cubic fold point for the full 'outer' problem

(5.1a,b,d) in which the hole is now replaced by a certain singularity condition at $r = 0$. The condition (5.1d) also is replaced by $\alpha = 2\pi \int_0^1 u^2 r dr$. Thus, to retain all the logarithmic corrections to the unperturbed cubic fold point parameters λ_{c0} and β_0, we *avoid* expanding the 'outer' solution in powers of $-1/\log[\epsilon d(\kappa)]$.

The form of the singularity condition for the solution to (5.1a,b,d) is found after constructing an infinite-order logarithmic expansion for the inner solution in the vicinity of the cooling rod. The far field behavior of this infinite-order expansion for the solution in the 'inner' region then yields the following singularity condition for (5.1a,b,d):

$$u = A\Big(1 - \frac{\log r}{\log z}\Big) + o(1), \quad \text{as } r \to 0. \tag{6.4}$$

The constant A , which depends on α, β and z is to be determined. Then the related problem is to determine the solution $u^*(r, \alpha, \beta, z)$, $\lambda^*(\alpha, \beta, z)$, and $A(\alpha, \beta, z)$ to

$$u^{*''} + \frac{1}{r}u^{*'} + \lambda^* F(u^*, \beta) = 0, \quad 0 < r < 1; \quad \alpha = 2\pi \int_0^1 (u^*)^2 r\, dr, \tag{6.5a}$$

$$u^{*'} + bu^* = 0, \quad \text{on } r = 1; \quad u^* = A\Big(1 - \frac{\log r}{\log z}\Big) + o(1), \quad \text{as } r \to 0. \tag{6.5b}$$

Here z is a parameter. For fixed z, the sums $\lambda_c^*(z)$ and $\beta_c^*(z)$ are the values of λ^* and β at which the related problem (6.5) has a cubic fold point. To determine the location of this cubic fold point, we simply append the side constraints $\lambda_\alpha^* = \lambda_{\alpha\alpha}^* = 0$ to (6.5). We refer to the curves $\lambda_c^*(z)$ and $\beta_c^*(z)$, obtained from (6.5), as 'universal' curves since they can be used for a cooling rod of arbitrary shape centered at the origin. To determine numerical values for $\lambda_c^*(z)$ and $\beta_c^*(z)$ corresponding to a cooling rod of a certain size and shape, we need only evaluate the product $z = \epsilon d(\kappa)$. Thus we have formulated a hybrid asymptotic-numerical method which has the effect of summing the logarithmic series (5.24) for the cubic fold point parameters. We emphasize that our method to treat these logarithmic series completely circumvents having to first compute all the coefficients λ_{ci} and β_i in (6.3).

There are several advantages in solving the related problem (6.5) numerically rather than proceeding with a direct numerical attack on the full problem (5.1). Foremost is that, for a cooling rod of arbitrary cross-section centered at the origin, $\lambda_c^*(z)$ and $\beta_c^*(z)$ are obtained by solving a boundary-value problem for ordinary differential equations. For this geometry, the 'exact' values $\lambda_c(\epsilon)$ and $\beta_c(\epsilon)$ can only be found by solving the partial differential equation (5.1). In addition, the curves $\lambda_c^*(z)$ and $\beta_c^*(z)$ can be re-used for a different hole geometry or a different value of κ simply by re-computing a *single* constant $d(\kappa)$. In contrast, once κ or the hole geometry is changed in the full problem (5.1), the *entire* curves $\lambda_c(\epsilon)$ and $\beta_c(\epsilon)$ must be re-computed by varying ϵ. Finally, we observe that (5.1) and (6.1) become increasingly difficult to solve as ϵ decreases. In contrast, after introducing the new variable v by

$$u^* = \frac{A}{\log z}(b^{-1} - \log r) + v, \tag{6.6}$$

the related problem (6.5) is not inherently stiff and can be easily solved for small values of ϵ.

To solve the related problem, it is more convenient to parameterize (6.5) by A rather than α. Substituting (6.6) into (6.5a,b), we obtain

$$v'' + \frac{1}{r}v' + \lambda^* F^{*0} = 0, \quad 0 < r < 1; \quad v' + bv = 0, \quad \text{on } r = 1, \tag{6.7a}$$

$$v = A\Big(1 - \frac{b^{-1}}{\log z}\Big) \quad \text{and} \quad v' = 0, \quad \text{at} \quad r = 0. \tag{6.7b}$$

Here we have defined F^{*0} by

$$F^{*0} \equiv F[v + A(b^{-1} - \log r)/\log z, \beta]. \tag{6.7c}$$

Next we form the extended system for (6.7) by taking derivatives of (6.7) with respect to A. The cubic fold point for (6.7) is determined by appending the side constraints $\lambda_A^* = \lambda_{AA}^* = 0$ to this extended system. Then the resulting problem, which is not stiff for small values of ϵ, is solved using COLSYS.

Finally, to estimate the error made in approximating $\lambda_c(\epsilon)$ and $\beta_c(\epsilon)$ by $\lambda_c^*[\epsilon d(\kappa)]$ and $\beta_c^*[\epsilon d(\kappa)]$, we must retain further terms in the far field expansion of the inner solution. A simple analysis shows that

$$\lambda_c(\epsilon) = \lambda_c^*[\epsilon d(\kappa)] + O\Big(\frac{\epsilon}{\log[\epsilon d(\kappa)]}\Big), \quad \beta_c(\epsilon) = \beta_c^*[\epsilon d(\kappa)] + O\Big(\frac{\epsilon}{\log[\epsilon d(\kappa)]}\Big). \tag{6.8}$$

We now give some results of the numerical computations for (6.1) and (6.7) when $F(u, \beta) = \exp[u/(1 + \beta u)]$.

In Figure 2a we plot the universal curves $\beta_c^*(z)$ versus z, obtained from (6.7), for

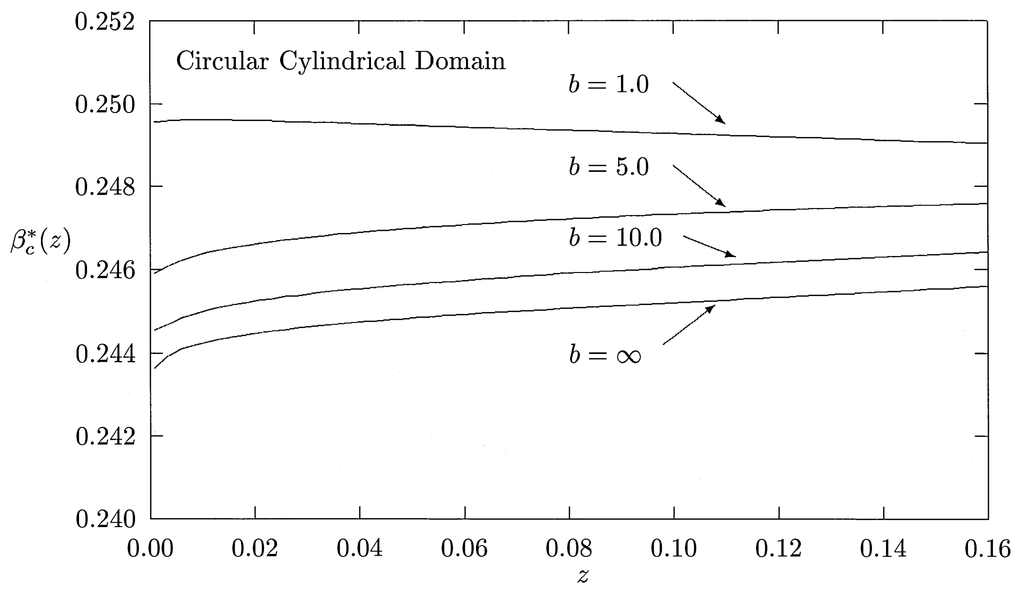

FIGURE 2a. Circular cylindrical domain containing a cooling rod of arbitrary cross-section centered at the origin: Plots of the universal curves $\beta_c^*(z)$ versus z for several Biot numbers b.

several values of b. The corresponding curves $\lambda_c^*(z)$ versus z are plotted in Figure 2b. Using the values of $d(\kappa)$ given in Appendix A, $\beta_c^*[\epsilon d(\kappa)]$ and $\lambda_c^*[\epsilon d(\kappa)]$ then are known

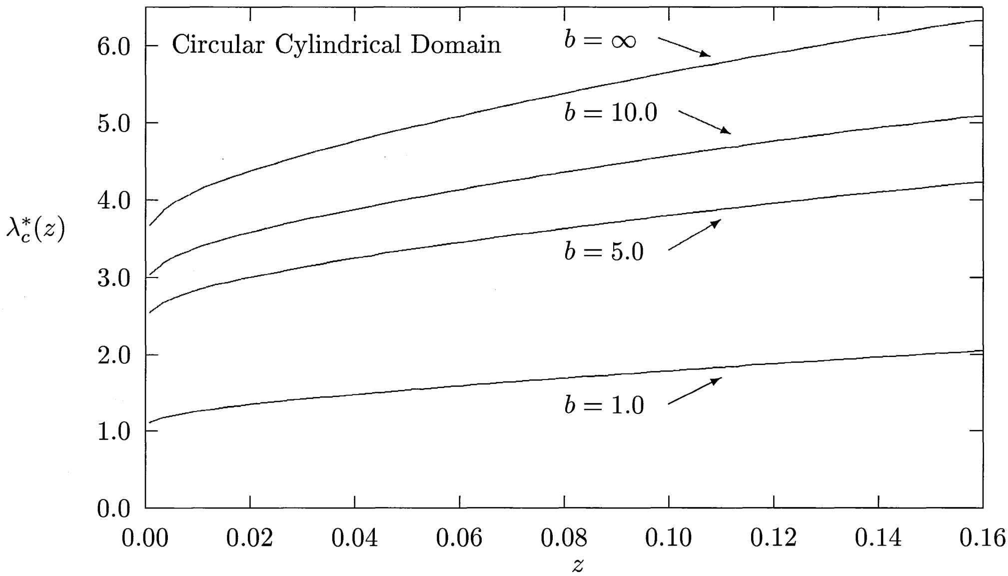

FIGURE 2b. Circular cylindrical domain containing a cooling rod of arbitrary cross-section centered at the origin: Plots of the universal curves $\lambda_c^*(z)$ versus z for several Biot numbers b.

explicitly for various κ and hole shapes.

In particular, consider an annular domain with inner radius ϵ and with $\kappa = \infty$ for which $d(\infty) = 1$. Then in Table 7a we compare the results for $\beta_c(\epsilon)$ obtained from the related problem (6.7), the full problem (6.1), and the two- or three-term expansions derived from (6.2). A similar comparison for $\lambda_c(\epsilon)$ is shown in Table 7b. From these tables we conclude, in general, that the sums $\lambda_c^*(\epsilon)$ and $\beta_c^*(\epsilon)$ of the logarithmic series are a better determination of $\lambda_c(\epsilon)$ and $\beta_c(\epsilon)$ than are the three-term expansions given in (6.2). However, we note that when $\epsilon = .1259$, the three-term expansion for $\lambda_c(\epsilon)$ is in closer agreement to the numerical result for $\lambda_c(\epsilon)$ than is $\lambda_c^*(\epsilon)$, although this is probably fortuitous.

ϵ	$\beta_c(\epsilon)(6.1)$	$\beta_c^*(\epsilon)(6.7)$	$\beta_c(\epsilon)(6.2b)$2 terms	$\beta_c(\epsilon)(6.2b)$3 terms
0.0009	0.24364	0.24364	0.24378	0.24377
0.0109	0.24426	0.24426	0.24471	0.24460
0.0259	0.24457	0.24457	0.24533	0.24515
0.0509	0.24484	0.24486	0.24606	0.24580
0.0759	0.24501	0.24505	0.24667	0.24633
0.1009	0.24514	0.24522	0.24724	0.24680
0.1259	0.24523	0.24538	0.24779	0.24725

TABLE 7a. Comparison of asymptotics and numerics for $\beta_c(\epsilon)$ in the case of a cooling rod concentric with a circular cylindrical domain with $b = \infty$ and $\kappa = \infty$.

For an annular domain with inner radius ϵ, the results for the cubic fold point parameters obtained from the related problem (6.7) also agree very closely with results

ϵ	$\lambda_c(\epsilon)(6.1)$	$\lambda_c^*(\epsilon)(6.7)$	$\lambda_c(\epsilon)(6.2a)$2 terms	$\lambda_c(\epsilon)(6.2a)$3 terms
0.0009	3.6803	3.6798	3.5809	3.6709
0.0109	4.1486	4.1486	3.8981	4.1148
0.0259	4.5023	4.4990	4.1093	4.4408
0.0509	4.9656	4.9421	4.3596	4.8586
0.0759	5.3907	5.3215	4.5693	5.2349
0.1009	5.8136	5.6636	4.7633	5.6044
0.1259	6.2494	5.9728	4.9510	5.9814

TABLE 7b. Comparison of asymptotics and numerics for $\lambda_c(\epsilon)$ in the case of a cooling rod concentric with a circular cylindrical domain with $b = \infty$ and $\kappa = \infty$.

obtained from the full problem for a wide range of κ. When $b = \infty$, in Figure 3a we plot the curves $\beta_c^*[\epsilon d(\kappa)]$ versus ϵ obtained from (6.7) for several values of κ. For this geometry $d(\kappa) = \exp[-1/\kappa]$. The selected numerical results for $\beta_c(\epsilon)$ obtained from the full problem (6.1) also are plotted in this figure. A similar comparison for $\lambda_c(\epsilon)$ is shown in Figure 3b. The close agreement between the results from the hybrid method and the results from the full problem for a wide range of κ and for moderately small values of ϵ is evident from these figures.

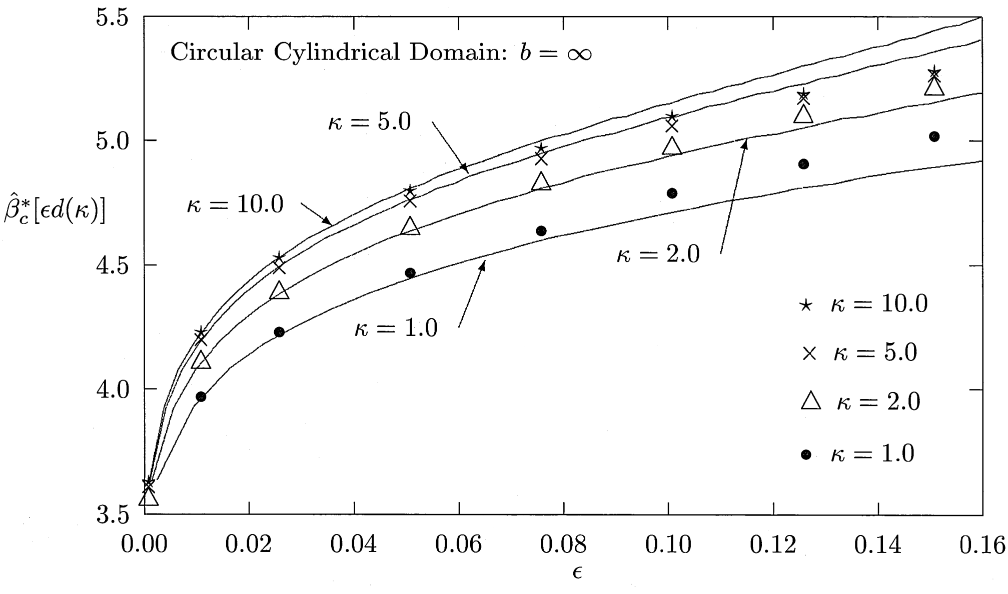

FIGURE 3a. Annular domain with inner radius ϵ and $b = \infty$: Plots of the curves $\hat{\beta}_c^*[\epsilon d(\kappa)]$ versus ϵ for several values of κ, where $\hat{\beta}_c^*[\epsilon d(\kappa)] \equiv (\beta_c^*[\epsilon d(\kappa)] - .24) \times 10^3$. Corresponding numerical results computed from (6.1) at selected values of ϵ are also shown.

For cooling rods of arbitrary cross-section centered at the origin, we anticipate a similar agreement between $\lambda_c(\epsilon)$ and $\lambda_c^*[\epsilon d(\kappa)]$ and between $\beta_c(\epsilon)$ and $\beta_c^*[\epsilon d(\kappa)]$ as for the case of an annular domain. Some related work in non-concentric geometries,

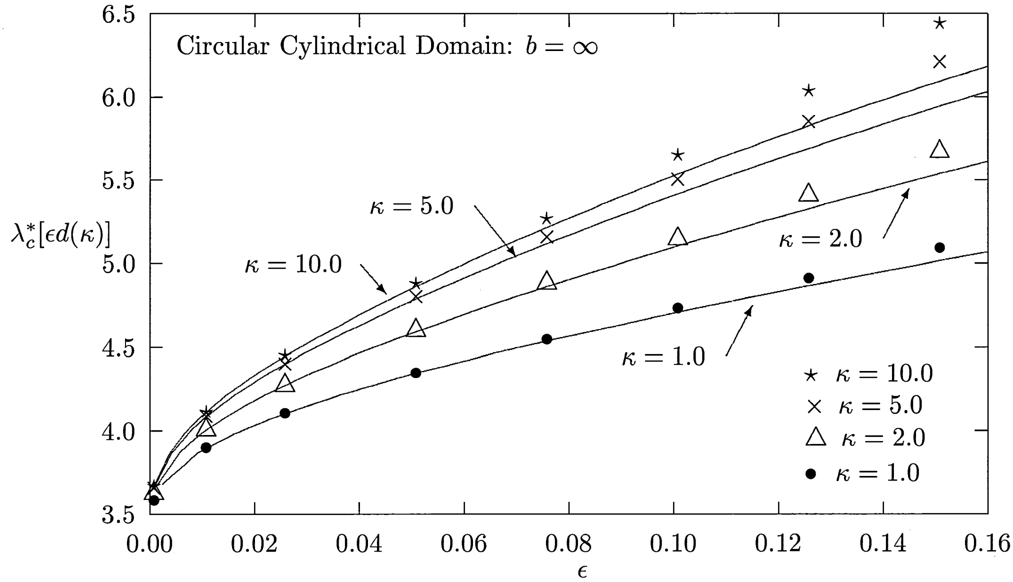

FIGURE 3b. Annular domain with inner radius ϵ and $b = \infty$: Plots of the curves $\lambda_c^*[\epsilon d(\kappa)]$ versus ϵ for several values of κ. Also shown, at selected values of ϵ, are the numerical results for $\lambda_c(\epsilon)$ from (6.1).

b	$\lambda_{c1}^*(5.33)$	$\beta_1^*(5.33)$	$\lambda_{c1}(5.28b)$	$\beta_1(5.28a)$
∞	11.167	0.04464	37.728	0.18787
10.0	8.3447	0.04134	23.058	0.14464
5.0	6.4455	0.03704	14.648	0.10986
3.0	4.9063	0.02911	8.8069	0.07072
1.0	2.7132	0.00996	2.2530	0.01227
0.50	2.1449	0.00444	0.9745	0.00312
0.25	1.8766	0.00203	0.4468	0.00077

TABLE 8. The coefficients for a cooling pellet or a spherical insulating pellet centered at the origin of a spherical domain.

which compared numerical results for (5.1) with the sum of a logarithmic series for a simple fold point, was done in [15].

6.3. Three dimensions: spherical domain. In the case of a spherical insulating pellet of radius ϵ, the expansions of $\lambda_c(\epsilon)$ and $\beta_c(\epsilon)$ are given in Proposition 5.3. The coefficients λ_{c1} and β_1 in these expansions are given in (5.28), in which the tensor P_{ij} is given by $P_{ij} = \delta_{ij}/2$. In the case of a cooling pellet, the expansions of $\lambda_c(\epsilon)$ and $\beta_c(\epsilon)$ are given in Proposition 5.4, where the coefficients λ_{c1}^* and β_1^* are given in (5.33). These coefficients are independent of κ and of the shape of the cooling pellet.

In Table 8 we give numerical values for the coefficients in the expansions of $\lambda_c(\epsilon)$ and $\beta_c(\epsilon)$ when a cooling pellet or a spherical insulating pellet is centered at the origin of a spherical domain. By combining the results in Table 1b and Table 8, the coefficients in the two-term expansions for $\lambda_c(\epsilon)$ and $\beta_c(\epsilon)$ are known for various κ, b, and hole shapes.

ϵ	$\lambda_c(\epsilon)(5.29)$	$\lambda_c(\epsilon)(6.1)$	$\beta_c(\epsilon)(5.29)$	$\beta_c(\epsilon)(6.1)$
0.010	5.0411	5.0411	0.23880	0.23880
0.025	5.0417	5.0417	0.23880	0.23880
0.050	5.0458	5.0457	0.23882	0.23882
0.075	5.0570	5.0565	0.23888	0.23887
0.100	5.0788	5.0767	0.23899	0.23896
0.125	5.1148	5.1088	0.23917	0.23908
0.150	5.1684	5.1549	0.23943	0.23925

TABLE 9. Comparison of asymptotics and numerics for an insulating pellet concentric with a spherical domain with $b = \infty$.

Suppose that a spherical insulating pellet of radius ϵ is centered at the origin. Then for $b = \infty$, in Table 9 we compare the two-term asymptotic result (5.29) for $\lambda_c(\epsilon)$ and $\beta_c(\epsilon)$ with corresponding numerical results obtained from the full problem (6.1). From this table we observe that the asymptotic results for $\lambda_c(\epsilon)$ and $\beta_c(\epsilon)$ are within .27% of the corresponding numerical results even when $\epsilon = .15$.

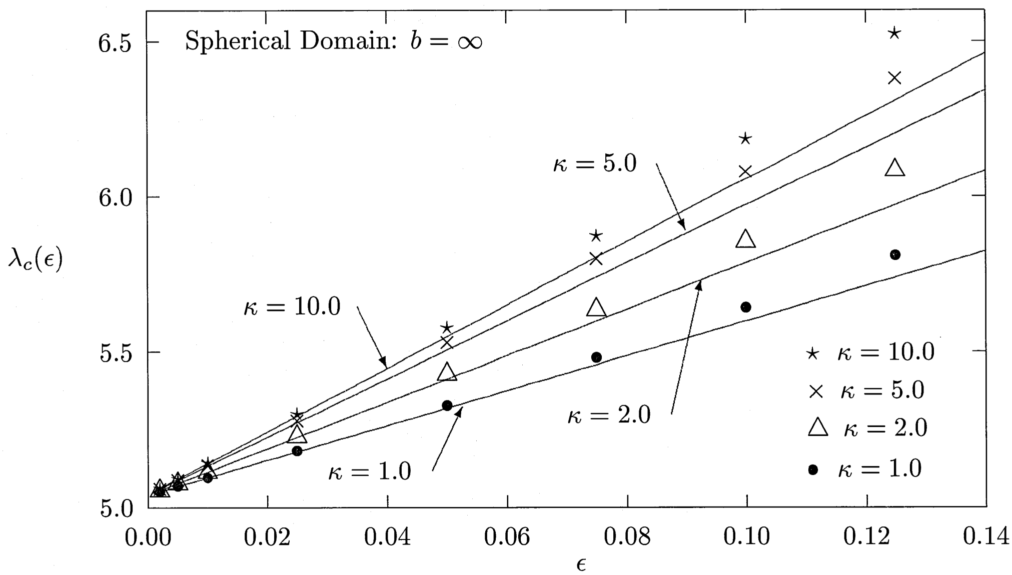

FIGURE 4. Concentric spheres with inner radius ϵ and $b = \infty$. For several values of κ, we compare the asymptotic results $\lambda_c(\epsilon)$ versus ϵ from (5.34) with the numerical results for $\lambda_c(\epsilon)$ from (6.1). The solid lines are the asymptotic results.

Now suppose that a spherical cooling pellet of radius ϵ, with $\kappa = \infty$, is centered at the origin. For this geometry, we have $C = 1$. Then when $b = \infty$, in Table 10 we compare the two-term results (5.34) with numerical results obtained from the full problem (6.1). The asymptotic results are not as good as for the case of an insulating pellet, but they are still within 5.6% of the numerical results even when $\epsilon = .15$. In Figure 4 we use the asymptotic result (5.34), and $C(\kappa) = \kappa/(1 + \kappa)$, to plot the curves $\lambda_c(\epsilon)$ versus ϵ for several values of κ. In this figure we also have shown selected

ϵ	$\lambda_c(\epsilon)(5.34)$	$\lambda_c(\epsilon)(6.1)$	$\beta_c(\epsilon)(5.34)$	$\beta_c(\epsilon)(6.1)$
0.002	5.0634	5.0635	0.23889	0.23889
0.005	5.0969	5.0973	0.23902	0.23901
0.010	5.1528	5.1541	0.23924	0.23922
0.025	5.3202	5.3287	0.23991	0.23978
0.050	5.5994	5.6354	0.24103	0.24057
0.075	5.8785	5.9642	0.24215	0.24123
0.100	6.1577	6.3183	0.24326	0.24178
0.125	6.4368	6.7012	0.24438	0.24225
0.150	6.7160	7.1165	0.24549	0.24266

TABLE 10. Comparison of asymptotics and numerics for a cooling pellet concentric with a spherical domain with $b = \infty$ and $\kappa = \infty$.

numerical results for $\lambda_c(\epsilon)$ obtained from (6.1). From this figure we observe that when $\epsilon \le .10$, the asymptotic result for $\lambda_c(\epsilon)$ closely approximates that for the full problem over a wide range of κ. A similar agreement is found for $\beta_c(\epsilon)$.

Acknowledgments. We would like to thank Prof. Joseph B. Keller for his helpful comments on the manuscript.

Appendix A. Computation of the logarithmic capacitance $d(\kappa)$

The constant $d(\kappa)$ is defined in terms of the solution to

$$\begin{gathered} \Delta v = 0, \quad y \notin D_1; \quad \partial_n v + \kappa v = 0, \quad y \in \partial D_1, \\ v = \log|y| - \log[d(\kappa)] + o(1), \quad \text{as } |y| \to \infty. \end{gathered} \tag{A.1}$$

Here ∂_n is the inward normal derivative to D_1 and D_1 contains the origin $y = 0$. For simplicity we restrict ourselves to star-shaped domains D_1 where $D_1 = \{y : r = |y| \le g(\theta)\}$. Here $g(\theta) > 0$ is a smooth 2π-periodic function and θ is the polar angle. After transforming (A.1) to a bounded domain, the constant $d(\kappa)$ was computed in [15] for elliptical and leaf-type domains whose boundaries are given by

$$\begin{gathered} g(\theta) = a[1 + (a^4 - 1)\sin^2(\theta)]^{-1/2}, \quad a > 0; \\ \text{ellipse with semi-axes } a, a^{-1}, \end{gathered} \tag{A.2a}$$

$$\begin{gathered} g(\theta) = \sigma + \frac{4}{3\sqrt{2}}[(3 - \sigma^2)^{1/2} - \sqrt{2}\sigma]\sin^2(n\theta), \quad 0 < \sigma \le 1; \\ \text{leaf with } 2n \text{ leaves.} \end{gathered} \tag{A.2b}$$

In (A.2b), n is a positive integer. For both classes of domains the area of D_1 is π. The results for $d(\kappa)$ found in [15] are summarized in the following tables:

κ	$a = 1.0$	$a = 2.0$	$a = 2.5$
∞	1.000	1.250	1.450
1	0.368	0.562	0.724

TABLE A.1. Logarithmic capacitance $d(\kappa)$ for the elliptical domain (A.2a).

κ	n	$\sigma = .25$	$\sigma = .75$
∞	2	1.267	1.068
∞	3	1.332	1.096
1	2	0.634	.4417
1	3	0.723	.4962

TABLE A.2. Logarithmic capacitance $d(\kappa)$ for the 'leaf' domain (A.2b).

References

1. J. Adler, *Criticality in a nearly circular cylinder* Proc. Roy. Soc. Lond. Ser. A, **411** (1987), 413–419.
2. U. Ascher, R. Christiansen and R. Russell, *Collocation software for boundary value ODE's*, Math. Comp., **33** (1979), 659–679.
3. E. Ash, B. Eaton and K. Gustafson, *Counting the number of solutions in combustion and reactive flow problems*, Z. Angew. Math. Phys., **41** (1990), 558–579.
4. T. Boddington, C. Feng and P. Gray, *Thermal explosions, criticality and the disappearance of criticality in systems with distributed temperatures. 1. Arbitrary Biot number and general reaction-rate laws*, Proc. Roy. Soc. Lond. Ser. A, **390** (1983), 247–264.
5. K. Fenaughty, A. Lacey and G. Wake, *Disappearance of criticality for small activation energy with arbitrary Biot number*, Combust. Flame, **45** (1982), 287–291.
6. P. Gray and P. Lee, *Thermal explosion theory*, Oxidation and Combust. Rev., **2** (1967), 1–183.
7. K. Gustafson and B. Eaton, *Exact solutions and ignition parameters in the Arrhenius conduction theory of gaseous thermal explosions*, Z. Angew. Math. Phys., **33** (1982), 392–405.
8. S. Kaplun, *Low Reynolds number flow past a circular cylinder*, J. Appl. Math. Mech., **6** (1957), 52–60.
9. W. Kordylewski, *Critical parameters of thermal explosion*, Combust. Flame, **34** (1979), 109–117.
10. P. A. Lagerstrom, *Matched Asymptotic Expansions—Ideas and Techniques*, Springer, New York, 1988.
11. C. Lange and H. Weinitschke, *Singular perturbations of limit points with application to tubular reactors*, Stud. Appl. Math., **84** (1991), 7–42.
12. I. Proudman and J. Pearson, *Expansions at small Reynolds number for the flow past a sphere and a circular cylinder*, J. Fluid Mech., **2** (1957), 237–262.
13. E. Van de Velde and M. J. Ward, *Criticality in reactors under domain or external temperature perturbations*, Proc. Roy. Soc. Lond. Ser. A, **434** (1991), 341–367.
14. M. J. Ward and J. B. Keller, *Nonlinear eigenvalue problems under strong localized perturbations with applications to chemical reactors*, Stud. Appl. Math., **85** (1991), 1–28.
15. M. J. Ward, W. Henshaw and J. B. Keller, *Summing logarithmic expansions for singularly perturbed eigenvalue problems*, SIAM J. Appl. Math., **53** (1993), 799–828.
16. M. J. Ward and E. Van de Velde, *The onset of thermal runaway in partially insulated or cooled reactors*, IMA J. Appl. Math., **48** (1992), 53–85.

DEPARTMENT OF MATHEMATICS, UNIVERSITY OF BRITISH COLUMBIA, VANCOUVER, BRITISH COLUMBIA, CANADA V6T 1Z2

ANALYTICAL APPLICATIONS DEPARTMENT, PARAMETRIC TECHNOLOGY, 128 TECHNOLOGY DRIVE, WALTHAM, MA 02154, U.S.A.